

Remediation of Thirdhand Tobacco Smoke with Ozone: Probing Deep Reservoirs in Carpets

Xiaochen Tang,* Clément Gambier, Nicolás López-Gálvez, Samuel Padilla, Vi H. Rapp, Marion L. Russell, Liana M. Klivansky, Raphael Mayorga, Charles Perrino, Lara A. Gundel, Eunha Hoh, Nathan G. Dodder, S. Katharine Hammond, Haofei Zhang, George E. Matt, Penelope J. E. Quintana, and Hugo Destaillats*



Cite This: *Environ. Sci. Technol.* 2023, 57, 9943–9954



Read Online

ACCESS |



Metrics & More



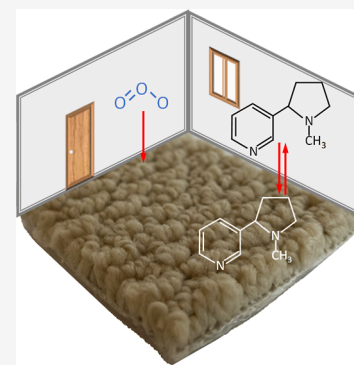
Article Recommendations



Supporting Information

ABSTRACT: We assessed the efficacy of ozonation as an indoor remediation strategy by evaluating how a carpet serves as a sink and long-term source of thirdhand tobacco smoke (THS) while protecting contaminants absorbed in deep reservoirs by scavenging ozone. Specimens from unused carpet that was exposed to smoke in the lab (“fresh THS”) and contaminated carpets retrieved from smokers’ homes (“aged THS”) were treated with 1000 ppb ozone in bench-scale tests. Nicotine was partially removed from fresh THS specimens by volatilization and oxidation, but it was not significantly eliminated from aged THS samples. By contrast, most of the 24 polycyclic aromatic hydrocarbons detected in both samples were partially removed by ozone. One of the home-aged carpets was installed in an 18 m³ room-sized chamber, where its nicotine emission rate was 950 ng day⁻¹ m⁻². In a typical home, such daily emissions could amount to a non-negligible fraction of the nicotine released by smoking one cigarette. The operation of a commercial ozone generator for a total duration of 156 min, reaching concentrations up to 10,000 ppb, did not significantly reduce the carpet nicotine loading (26–122 mg m⁻²). Ozone reacted primarily with carpet fibers, rather than with THS, leading to short-term emissions of aldehydes and aerosol particles. Hence, by being absorbed deeply into carpet fibers, THS constituents can be partially shielded from ozonation.

KEYWORDS: fast mobility particle sizer, ultrafine particles, PAHs, VOCs, GC/MS



INTRODUCTION

Thirdhand smoke (THS) is the residual chemical contamination left behind by tobacco use.^{1,2} This pervasive indoor pollution can linger in homes for years after regular smoking stopped and is difficult to remove with conventional cleaning methods.^{3,4} Some indoor materials become deep THS reservoirs, resulting in long-term re-emissions of contaminants to indoor air and contamination on surfaces. Among the different materials with which smoke is in direct contact, carpets can be considered major THS sinks and long-term emission sources. Singer et al.⁵ showed that in a room-sized chamber where cigarettes were machine-smoked under controlled conditions, the postsmoking gas-phase concentration of nicotine was significantly reduced (by up to 45%) in experiments with wall-to-wall carpet compared with identical conditions with stainless-steel floors. By contrast, in the same tests, the concentrations of co-emitted volatile tobacco compounds that do not adsorb to surfaces, such as benzene and acrylonitrile, were not affected by the presence of carpet. Similar experiments in which repeated cycles of daily smoking took place over a month showed that accumulation of nicotine and other semivolatile tobacco compounds in indoor materials

resulted in increasingly strong re-emission and rising background concentration of THS semivolatile pollutants in chamber air.⁶ In environments where smoking takes place regularly, carpets and other materials can become severely contaminated with THS, leading to exposures by inhalation, dust ingestion, and dermal contact.⁷

Delivering high concentrations of ozone in unoccupied residential and commercial buildings is usually implemented to remove offensive odors from tobacco use, fire damage, or mold and for disinfection purposes.⁸ Ozone generators are regularly used by hotel operators and rental car companies to “freshen up” rooms and vehicles.⁹ While the primary goal of ozonation is odor control, it is often implicitly believed that the treatment also results in healthier indoor environments. However, the effectiveness of ozonation in de-polluting the treated areas is

Received: February 28, 2023

Revised: June 11, 2023

Accepted: June 12, 2023

Published: June 27, 2023



not well-documented. Ozone reacts primarily on material surfaces, with semivolatile contaminants that partition to indoor materials, and it can also react in the gas phase with alkenes and other reactive compounds.¹⁰ Laboratory tests showed that the reaction of nicotine with ozone produced ultrafine particles and oxygenated byproducts that have a higher asthma hazard index than their precursor.¹¹ On carpet, ozone reacts with polymers, coatings, and dyes present in the fibers, releasing *n*-aldehydes and unsaturated aldehydes.^{12–20} Such reactions were shown to induce permanent chemical changes in nylon, polyester, and other fibers, with the incorporation of oxygen to form –OH and –COOH functional groups, affecting surface wettability and mechanical properties.²¹

In a recent study, we evaluated the ozonation of a room-sized chamber 24 h after a smoking event and found that the treatment could partially remove surface-bound THS contaminants such as nicotine and polycyclic aromatic hydrocarbons (PAHs) while also producing volatile byproducts and ultrafine particles that remained airborne several hours after treatment ended.²² That study was limited by the fact that the THS constituents removed by ozone had been released and adsorbed to indoor surfaces only a few hours prior to treatment. Another limitation was the absence of carpet, a material that represents approximately 50% of the US residential flooring market, and on which fast ozone deposition provides a scavenging effect comparable to ventilation, with an estimated air exchange rate (AER) of $\sim 0.4 \text{ h}^{-1}$.²³ Here, we expand the scope of our analysis by studying the ozonation of THS deposited on unused carpets and on aged carpets retrieved from smokers' homes to assess the role of deep reservoirs in protecting THS contaminants from oxidation by ozone.

MATERIALS AND METHODS

Aged Carpet from THS-Contaminated Homes. THS-contaminated carpets were retrieved from homes in the San Diego metropolitan area, recruited as part of the Healthy Homes—5 (HHS) study led by San Diego State University.²⁴ A prescreening process assessed the home contamination levels by collecting surface wipe samples from walls, doors, and built-in cabinets, extracting the samples, and determining nicotine by gas chromatography/mass spectrometry (GC/MS) following an established methodology.^{25,26} Homes selected for the HHS study had high nicotine surface loading above $10 \mu\text{g m}^{-2}$ on average within the home, taken as a threshold for a high level of THS contamination. This threshold was the geometric mean of surface nicotine concentration in nonsmoking homes known to have been previously occupied by smokers.²⁷ Homes at or above $10 \mu\text{g m}^{-2}$ were selected because a significant level of contamination was required in order to examine the effects of deep cleaning. A subset of four homes (named A–D) was selected for the carpet ozonation tests reported here. Airborne nicotine concentrations were sampled before removing the carpet by drawing room air through fiberglass filters coated with sodium bisulfate held in open-face filter holders, following the Hammond method.²⁸ Details on home selection criteria and the experimental methods used for surface wipe and air nicotine samples are described in Section S1 (Supporting Information). Measured nicotine surface loading and indoor air concentration at each home are reported in Table S1, with surface levels between 0.78 and 79 mg m^{-2} and airborne concentrations between 0.24 and $3.6 \mu\text{g m}^{-3}$. Carpets for

ozonation tests were retrieved from homes between January 2021 and April 2022, wrapped in plastic, and shipped to LBNL for further experimental work. The carpets were characterized as described in Section S2. In two cases (homes A and B), the removed carpet consisted of two layers, with a top sheet applied over a padded backing layer, as illustrated in Figure S1. Three of the four homes were vacant during sampling and carpet removal. They had been occupied by smokers over the previous 6–25 years, and the retrieved carpets had been installed during most of that time.

Preparation of Fresh THS in New (Clean) Carpet. A reference set of “fresh THS” samples was prepared by depositing tobacco smoke onto unused and clean carpet specimens corresponding to the top and backing layers. Both the clean carpet top layer and the clean backing were procured, stored in a smoke-free laboratory prior to their use in experiments, and characterized as described in Section S2. Tobacco smoke was generated by smoldering cigarettes inside a cubic Teflon-lined 150 L chamber, in which square carpet specimens of $7.5 \times 7.5 \text{ cm}$ were placed facing upward on the bottom of the chamber, away from the cigarettes. The specimens remained in contact with the smoke for 24 h. The amount of smoke produced was adjusted by consumption of between $\frac{1}{4}$ and 3 cigarettes (Camel 99s Turkish Domestic Blend). Laboratory air was introduced continuously into the chamber and was mixed efficiently by the operation of four miniature fans. The fresh THS generation system is illustrated in Figure S2, and the chamber air exchange rate (AER = 0.5 h^{-1}) was determined by following CO_2 concentration decay, as described in Section S3.

Ozonation of Carpet in Bench-Scale Tests. The small-scale chamber enabled investigation of the chemistry between ozone and THS on carpets under different conditions in a short time frame (3–4 h) and allowed us to test and compare across multiple experimental variables, including THS loading, ozone level, relative humidity (RH), and type and age of carpets. A schematic of the bench-scale apparatus used for these tests is presented in Figure S3. A stream of filtered laboratory air was split into two air flows, adjusted by mass flow controllers (Alicat Scientific) to 0.7 and 0.3 L min^{-1} , respectively. The first stream was saturated with water in a bubbler (humidifier) or, alternatively, delivered directly to the system through a bypass. The other stream circulated through an ozone generator of adjustable output (UVP Pen-Ray, Analytik Jena). Both streams were joined at the inlet of a cylindrical exposure Teflon chamber (7.5 cm diameter, 12 cm height) in which a carpet specimen was placed at the bottom. The AER was 1.9 min^{-1} . The target ozone concentration was 1000 ppb, and it was measured continuously either from the inlet or at the chamber exhaust using a photometric detector (model 202, 2BTech). Temperature and RH were measured by a HOBO Temp/RH sensor and Data Logger (U23-002 Pro v2, Onset). Experiments were conducted at three different RHs: dry (<1% RH), 13% RH, and 72% RH, all at room temperature (21–23 °C). Each carpet specimen used in these tests was cut from the center of a square, as described in Figure S4. The excess material from the edges was extracted to determine pre-ozonation baseline levels. After ozonation, the exposed material was cut into four equivalent quarters, two of which were used for duplicate determinations. Both pre- and post-ozonation materials were extracted with methanol or with a 1:1 acetone/hexane mixture to determine nicotine or PAH loading, respectively, as described in Section S4. Bench-scale

tests were carried out using both aged THS-laden carpets (retrieved from the field) and fresh THS specimens prepared in the laboratory. A subset of these samples was also sent to UC Riverside for additional chemical composition measurements to examine ozonation byproducts, as described in Section S5.

Ozonation of Aged Carpet Installed in a Room-Sized Chamber. A 37 day long experiment was carried out in an 18 m³ room-sized chamber at LBNL built with gypsum wallboard and vinyl flooring, which was described previously.²² The chamber has a very low VOC background from building material emissions and a persistent but low nicotine background due to multiple smoking experiments carried out over many years. The AER of the chamber (0.5 h⁻¹) was measured at the beginning and the end of the experiment by CO₂ decay, as described in Section S3. Ozone was produced at various times during the experiment with a commercially available generator (Airthereal MA 10k PRODIGI) that was placed in the center of the chamber. This generator delivers up to 10 g O₃ per hour, which is a significantly higher output than that from the unit used in our previous experiments.²² The experimental timeline is presented in Tables S2 and S3. Briefly, the carpet retrieved from home A (5 m² of carpet top and backing, 7–8 years of exposure to smoke) was installed in the chamber at the beginning of the experiment ($t = 0$) and was left in the same position for 35 days. Background measurements were taken two days before installing the carpet to record initial chamber conditions and after releasing ozone using the generator one day before installing the carpet to assess emissions from ozonating the chamber materials. Once installed, the carpet was allowed to equilibrate with the chamber over 11 days, during which several samples were taken (“carpet background”). At $t = 11$ d, an initial amount of ozone was released, and measurements were taken over the next six days (“1st carpet ozonation”). At $t = 17$ d, a second ozonation was carried out by delivering a significantly larger amount of ozone, with measurements performed in the two days following that event (“2nd carpet ozonation”). In order to evaluate the interaction of carpet with fresh smoke, at $t = 19$ days, six cigarettes were smoked inside the chamber (three units of Camel 99s Turkish Domestic Blend and three Marlboro Special Blend Smooth Mellow Flavors) under identical conditions to those in our previous study. Measurements were carried out on the next day ($t = 20$ d) to characterize THS, and the ozone generator was operated immediately after sampling. Samples were taken during the 12 days following ozonation (“3rd carpet ozonation”), followed by a second ozonation event, and subsequent sampling was carried out in the ensuing two days (“4th carpet ozonation”). Samples collected during each experimental period included (a) airborne nicotine with the Hammond method; (b) VOCs using sorbent tubes and DNPH-coated silica cartridges; (c) aerosols using a fast mobility particle sizer (FMPS), an optical particle sizer (OPS), and an aerosol particle sizer (APS); and (d) 10 × 10 cm specimens of the carpet top and backing from two different areas of the carpet (labeled “X” and “Y”). Removing these small samples did not reduce the total carpet area by more than 2.5% at the end of the experiment. The details of the sampling and analytical methods are described in Section S6.

RESULTS AND DISCUSSION

Characterization of Unused and Aged Carpet. Table S1 summarizes the physical and chemical characterization of aged carpet samples. For these, as well as for the unused fresh carpet samples, the top layers were made with either twist (cut) or loop pile, which are the most popular styles for wall-to-wall carpeting in the US. The backing was made of bonded polyurethane foam. The fiber volume was 89 mm³ for the unused carpet and between 35 and 439 mm³ for the four aged carpets. Spectra collected with attenuated total reflectance-Fourier transform infrared (ATR-FTIR) spectroscopy allowed us to verify that aged carpets from homes A, B, and C, as well as the unused carpet, were primarily made with nylon fibers, and the carpet from home D was made with polypropylene fibers.²⁹ The aged backing, as well as the unused backing materials, was made with small pieces of polyurethane bonded with a polymeric adhesive. Figure S5 illustrates the ATR-FTIR spectra obtained for some of these samples.

The nicotine loading was determined by extracting each carpet specimen with methanol before ozonation. In unused carpet exposed to the smoke of one cigarette (“1-cig” test), it was 155 ± 47 and 140 ± 50 mg m⁻² for the carpet top and backing, respectively. When a specimen of the same unused carpet top was exposed to the smoke of three cigarettes (“3-cig” test), the loading was 190 ± 27 mg m⁻². The relative standard deviation (RSD) of these determinations was 30, 36, and 14%, respectively. These values are comparable to those determined for the aged carpet retrieved from home B, which had the highest nicotine loading among carpets from all four homes, 164 mg m⁻² (RSD <10%), comprising the sum of the top and the backing. As shown in Table S1, the highest carpet nicotine loading in home B coincided with the highest concentrations of nicotine in the air, surface, and dust (expressed in mass units), compared to the other homes. Carpets from homes A and C were made of similar materials and had comparable nicotine loadings, while those homes also had similar air, surface, and dust nicotine levels. It should be noted that nicotine loadings determined from the extraction of a whole carpet specimen were between one and 3 orders of magnitude higher than the loading calculated from the analysis of dust vacuumed from the same carpet. By contrast, nicotine was not detected in the carpet retrieved from home D, despite relatively high levels being found in indoor air and surface wipes. Dust concentrations were also significantly lower than in the other three homes. The fact that the carpet was made of polypropylene rather than nylon may be one of the reasons for the observed differences.

Bench-Scale Chamber Results. Ozone Consumption vs Nicotine Loading. Figure S6 illustrates typical ozone concentrations recorded during bench-scale experiments. Ozone consumption was observed in all tests, with levels immediately dropping to 200–400 ppb from ~1000 ppb when entering the chamber containing the carpet specimen and then slowly reducing the gap with incoming ozone to 100–300 ppb within 1 h. During the remaining reaction time, the ozone level was constant. The average mass of ozone consumed in reactions with the carpet and with THS present in the carpet over an ozonation period τ was calculated as

$$\Delta m_{\text{O}_3}^{\tau} = \frac{\int_0^{\tau} [C_{\text{inlet}} - C(t)] \times Q \, dt}{\tau} \quad (1)$$

where C_{inlet} is the average ozone concentration measured at the inlet during the experiment, $C(t)$ is the outlet concentration recorded as a function of time, and Q is the air flow rate. Figure S7 illustrates the results obtained for different carpet samples. Even in the absence of carpet, there was a residual amount of ozone reacting with chamber walls and tubing. With clean (THS-free) carpet top, the ozone consumed over $\tau = 3.1$ h was $\Delta m_{\text{O}_3}^\tau = 0.20 \mu\text{mol h}^{-1}$, and it increased to $0.87 \mu\text{mol h}^{-1}$ for field carpet B (1.70 μmol nicotine loading, $\tau = 3.5$ h), following a nearly linear trend that comprised intermediate values for field sample A ($\tau = 3.3$ h) and clean carpet exposed to the smoke of a quarter of a cigarette (1/4-cig, $\tau = 4.0$ h). However, for clean carpet exposed to smoke from smoldering a whole cigarette (1-cig, $\tau = 3.5$ h) and three cigarettes (3-cig, $\tau = 3.1$ h), the ozone consumption reached a plateau around $0.7 \mu\text{mol h}^{-1}$, which was not proportional to the amount of nicotine present in the surface.

The same results were used to calculate the ozone deposition velocity v_τ on carpet surfaces, as^{13,15}

$$v_\tau = \frac{Q}{C_{\text{avg}}^\tau \times A} \times (C_{\text{inlet}} - C_{\text{avg}}^\tau) \quad (2)$$

where C_{avg}^τ is the average ozone level exiting the chamber over a period of duration τ and A is the surface area of the carpet specimen. The deposition velocity was calculated in each case for the whole duration of individual tests (in the range of $\tau = 1.8$ – 4.1 h) and also for the initial hour, during which the uptake was fastest, as shown in Figure 1. It should be noted

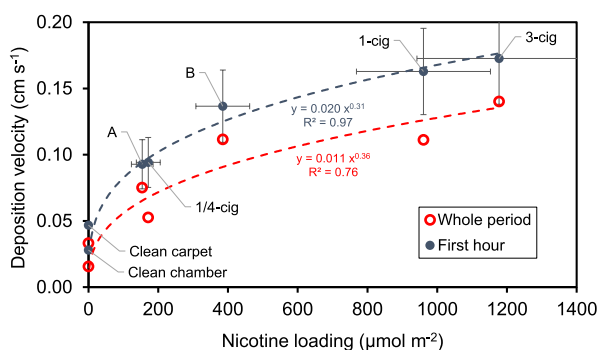


Figure 1. Ozone deposition velocity as a function of nicotine loading in bench-scale experiments. (A) Aged carpet retrieved from home A; (B) aged carpet retrieved from home B; 1/4-cig: new carpet exposed to the smoke from one-quarter cigarette; 1-cig: new carpet exposed to the smoke from one cigarette; and 3-cig: new carpet exposed to the smoke from three cigarettes.

that ozone reacted with not only nicotine but also other coexisting THS chemicals and with the carpet itself. The ozone deposition velocity v_τ increased as the THS loading increased, suggesting that at least a fraction of the THS compounds present in the sample were available for ozonation. The data in Figure 1 could be fit to a simple model with an exponent of 0.31 for the first hour test and 0.36 for the whole period, suggesting a transition to a mass-transfer limited regime. The fitted equations are included in Figure 1.

Nicotine Removal Efficiency. In each test, the nicotine removal efficiency (RE_N , %) was calculated as

$$RE_N = \left[\frac{(N_0) - (N_\tau)}{(N_0)} \right] \times 100 \quad (3)$$

where (N_0) and (N_τ) are the loading of nicotine measured initially and at time τ , respectively. Tests were carried out with the ozone generator turned off (“conditioning”) and turned on (“ozonation”) to account for the evaporative loss of nicotine and its reaction with ozone, respectively. These results are presented in Figure 2.

Conditioning of 1-cig carpet specimens (Figure 2a) at 13% RH showed noticeable nicotine removal, corresponding to $RE_N = 56\%$ for the carpet top and 11% for the backing. Compared with the removal efficiencies measured during ozonation, the nicotine removal attributed to ozone (calculated as the difference between conditioning and ozonation) was 30% for the backing and negligible for the carpet top (in the order of the experimental error of the measurements). For carpet top exposed to the smoke of 3 cigarettes (Figure 2b), conditioning had a smaller effect than ozonation, corresponding to $RE_N = 10\%$, while the net removal attributed to ozone was 39% at 13% RH. In aged carpets from homes A and B (Figure 2c,d), no significant nicotine removal was observed, with calculated efficiencies fluctuating around 0% in most cases. Both field-aged samples, including both top and backing layers, were placed in the chamber with air at different RHs (dry, 13%, and 72%) flowing through the chamber for 17 h before the ozonation started. Changes in RH did not affect ozone surface reactivity, which is consistent with previously reported observations.³⁰ The negative RE_N values in a number of cases suggested transport of nicotine from the top to the backing rather than removal by evaporation or ozonation. These results could also be attributed to uneven distribution of nicotine among the specimens, considering the 14–36% RSD determined for nicotine loading. Despite the substantial fluctuations observed in these tests, it is clear that the large amounts of nicotine absorbed in aged carpet were not lost in a significant way by either evaporation or ozonation. This result is qualitatively different from those from fresh THS deposited on new carpet specimens, as shown in Figure 2a,b, in which “accessible” surface-bound nicotine could be partially removed by volatilization and reaction with ozone.

PAH Removal Efficiency. In separate tests, we determined the surface loading of 26 PAHs present in the carpet specimens corresponding to blank (clean) carpet top material without THS, clean carpet that was exposed to the smoke of three cigarettes in the lab (3 cig), and aged carpet retrieved from home B. The results are summarized in Table S4. A non-negligible PAH loading was measured in THS-free carpet (total PAH = $246 \mu\text{g m}^{-2}$), as these compounds are ubiquitous in the environment and were shown to be present in dust collected from carpet.^{31–34} The fresh and aged THS specimens had 6 and 17 times higher total PAH loading, respectively, suggesting that tobacco smoke was a major source of these contaminants, consistent with measurements of PAHs in settled house dust from 132 California homes.³³ The total PAH loading reported here, determined from whole carpet extraction, is between 1 and 2 orders of magnitude higher than the amounts reported in the literature from the analysis of dust collected by vacuuming carpets.^{33,34} This is consistent with our above-mentioned observation for nicotine loading.

In the samples containing THS, the removal efficiency for each of them (RE_{PAH}^i , %) was calculated as

$$RE_{\text{PAH}}^i = \left[\frac{(\text{PAH}_0^i) - (\text{PAH}_\tau^i)}{(\text{PAH}_0^i)} \right] \times 100 \quad (4)$$

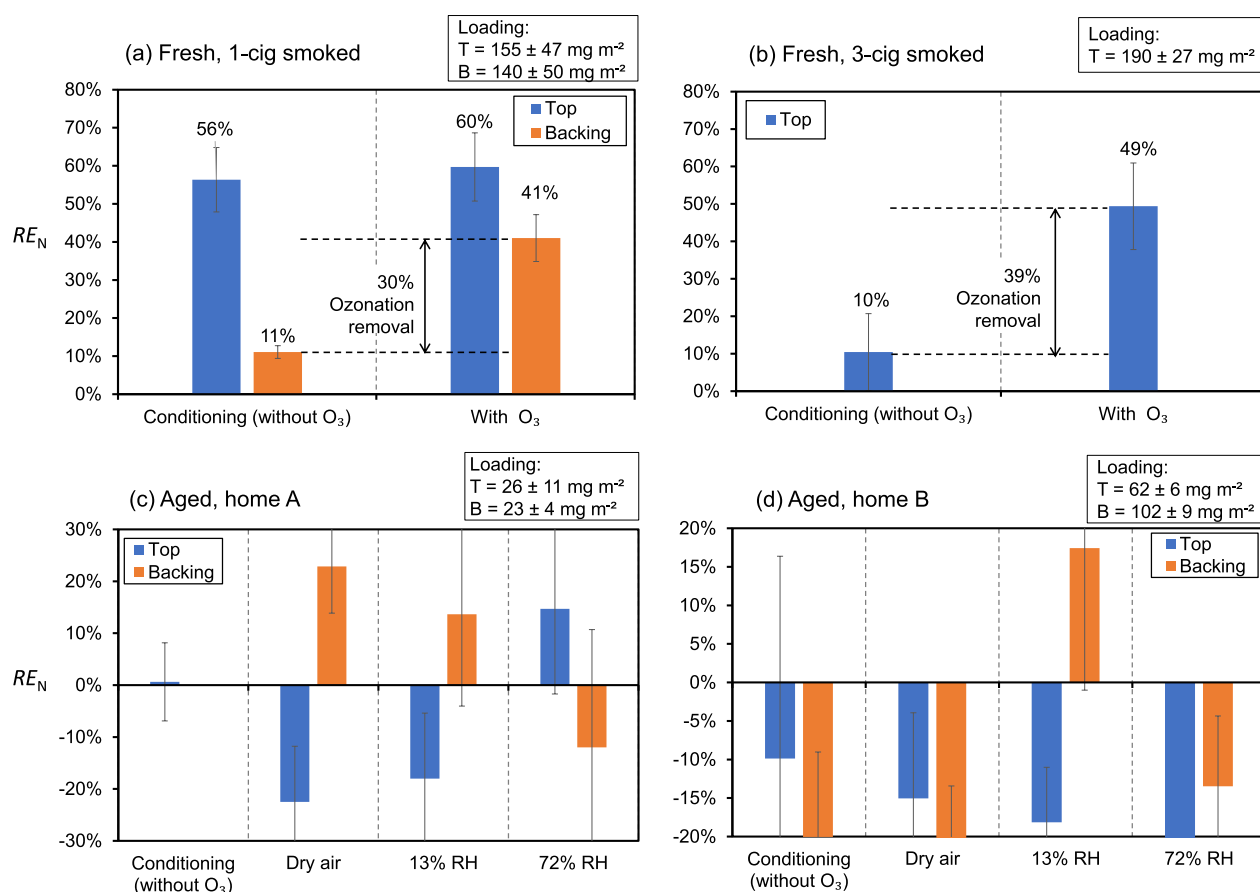


Figure 2. Nicotine removal efficiency of (a) lab-generated 1-cig sample; (b) lab-generated 3-cig sample; (c) aged carpet from home A; and (d) aged carpet from home B.

where (PAH_0^i) and (PAH_τ^i) are the surface loading of the i -th PAH measured initially and at time τ , respectively. Figure 3 illustrates (PAH_0^i) and (PAH_τ^i) for a majority of the PAHs, with vapor pressure below 0.001 mmHg. These analytes are likely removed exclusively through reaction with ozone due to their low volatility. In almost all the cases, there was a net removal of PAHs that can be attributed to ozonation, with RE_{PAH}^i values spanning from negligible (comparable to the relative error of the determinations, $\approx 15\%$) to 100% elimination. Removal of PAH by ozonation in aged carpets did not follow the same trends as those reported above for nicotine, suggesting that PAHs are more accessible and susceptible to reaction with ozone. One possible reason for a higher availability of PAHs is the fact that these compounds deposit onto the surface as constituents of aerosol particles and are unlikely to diffuse deeply into the carpet fibers due to their low volatility. Ozonation likely resulted in the formation of oxy-PAHs, hydroxy-PAHs, and/or quinones,³⁵ but our analytical method did not have enough sensitivity for the detection of these potential byproducts.

We further illustrate these observations by reporting separately in Figure S8 the results corresponding to benzo(*a*)pyrene [B(*a*)P], a PAH of particular concern because it is listed in IARC Group 1 as a known carcinogen. B(*a*)P was removed from both the 3-cig and home B carpet samples, with $RE_{PAH}^{B(a)P} = 81$ and 43%, respectively. Despite the lower removal efficiency in the aged sample, the absolute amount of B(*a*)P eliminated was more than twice that from fresh THS. These results suggest that ozonation can be effective in the

elimination of harmful THS contaminants from carpet. Further evaluation is needed to assess the trade-offs between removing B(*a*)P and other PAHs and the likely formation of hydroxy-PAHs and other harmful byproducts that could not be analyzed in this study.

Additional Analytes Detected by High-Resolution Mass Spectrometry. Methanol extracts of specimens from fresh THS (3-cig sample) and aged THS (carpet from home B) before and after ozonation were analyzed with electrospray ionization time-of-flight-mass spectrometry (ESI-MS) in the positive ion mode. Tentative chemical formula identifications were made by elemental formula assignment and are presented in Table S5. Confident structure identification was challenging due to the lack of authentic standards. In general, more chemical species were detected in the field carpet extracts than in the 3-cig sample, with a m/z range of 44–800. Nicotine was detected in all extracts, while possible nicotine oxidation byproducts¹¹ such as cotinine ($C_{10}H_{12}N_2O$), nicotine *N*-oxide ($C_{10}H_{14}N_2O$), and nicotinamide ($C_6H_6N_2O$) were only seen in the field carpet extracts. Not surprisingly, nylon cyclic dimer ($C_{12}H_{22}N_2O_2$) was also present in both carpet samples. However, potential nylon oxidation products ($m/z = 422.44$, 718.89, and 746.94) were only observed in the postozonation field carpet extract, suggesting that they may have been formed by reaction with ozone. Other chemicals detected in the field carpets include dodecyl sulfate ($C_{12}H_{26}O_4S$), palmitate ($C_{16}H_{32}O_2$), and stearic acid ($C_{18}H_{36}O_2$), which may originate from cooking and household cleaning products.

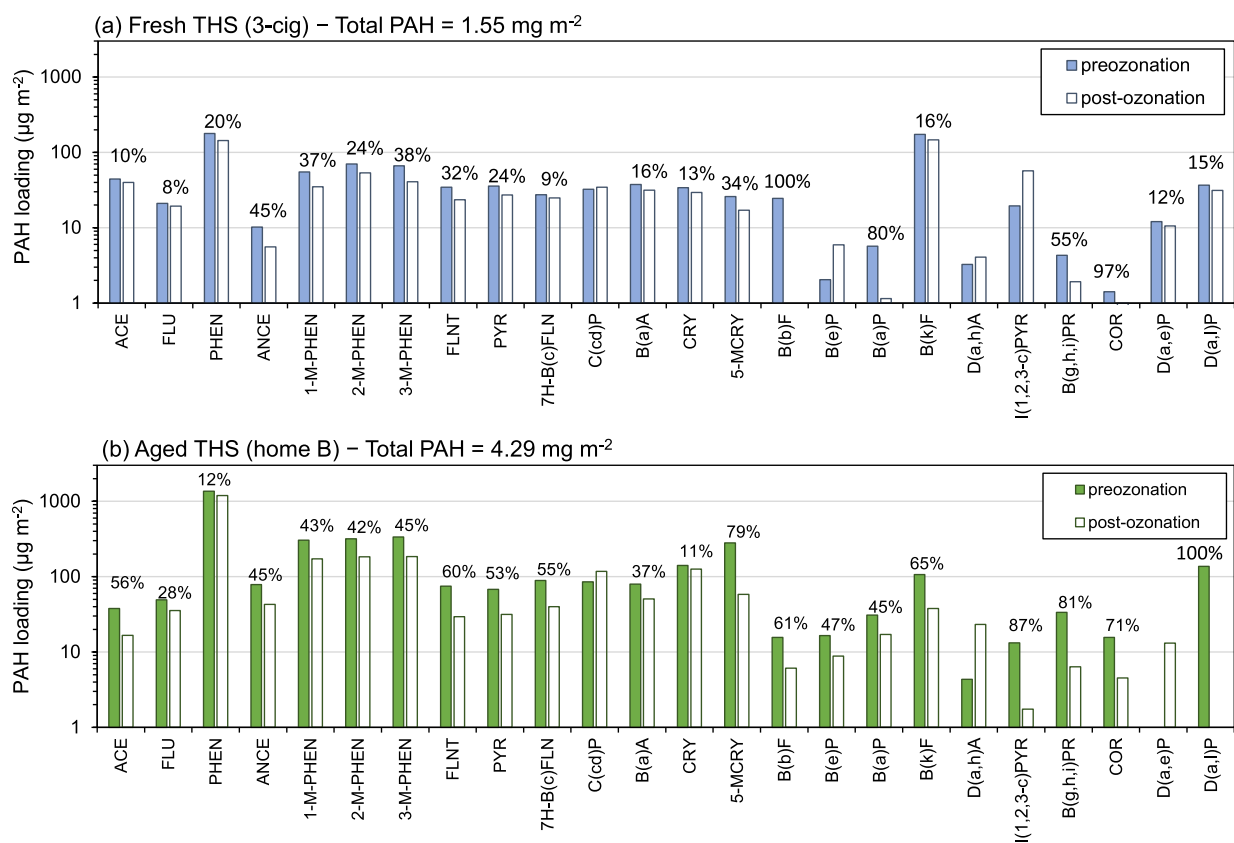


Figure 3. PAH surface loading before and after ozonation. (a) Lab-generated carpet sample exposed to the smoke of three cigarettes; (b) aged carpet retrieved from home B.

To further study the nitrogen-containing chemicals with higher detection sensitivity, a fraction of each carpet specimen (~ 500 mg) was heated to 100 °C over 15 – 20 min. Evaporative emission was measured in a flow chamber with chemical ionization time-of-flight mass spectrometry (CIMS) using iodide (I^-) as the reagent ion. A total of eight N-containing chemicals (Table S5) were detected in emissions from all four specimens, indicating that these oxidized chemicals may be present in tobacco smoke before experiencing ozonation.

Room-Sized Ozonation Chamber Results on Aged THS. Ozone Concentration. The results corresponding to each of the five time periods in which the ozone generator was used are presented in Figure S9. In the chamber background ($t = -1.2$ d) and first carpet ozonation ($t = 11$ d), the generator was operated for 6 min and turned off as soon as the concentration exceeded 1 ppm, having delivered 200 mg of ozone. The corresponding curves are presented in Figure S9a, showing a gap between them, illustrating that a large amount of ozone reacted with carpet, leading to a faster ozone decay rate. Figure S9b displays three very similar curves corresponding to subsequent ozonation periods in which the chamber target concentration was increased to 10 ppm. This mark was achieved by delivering 1.6–1.7 g of O_3 over a period of 48–51 min during the second ozonation ($t = 17$ d), and the two ozonation periods performed after fresh smoke were generated at $t = 19.7$ and 33.7 d.

Nicotine in Room Air. Results presented in Figure 4a and Table S2 show the impact of the presence of a THS-laden carpet on airborne nicotine concentrations. A relatively low level of nicotine (1 – 3 ng m^{-3}) was present in the chamber due

to residual THS on chamber surfaces from previous experiments. However, nicotine levels increased by 1 order of magnitude once the carpet was installed and remained relatively constant for 10 days during the carpet equilibration period with the chamber, with an average level of 22 ± 6 ng m^{-3} during the “carpet background” period. This result illustrates the role of the contaminated carpet as a secondary THS source. The first ozonation did not result in a significant reduction of nicotine levels, and the second ozonation, with a significantly higher oxidative power, led to a reduction of 59% with respect to the average carpet background level. Our experimental timeline did not allow us to follow the evolution of airborne nicotine for a longer period following the second ozonation to explore possible recovery of the carpet source strength. On $t = 19$ d, a measurement made 14 h after the smoking event showed a high nicotine concentration of 1.17 ± 0.09 µg m^{-3} . While most of the freshly emitted smoke was removed by seven ventilation air exchanges at the time of sampling, the high airborne nicotine level reflected the presence of new THS sources on all chamber surfaces, not only the carpet. Upon ozonation, airborne nicotine decreased rapidly, dropping by 1 order of magnitude, illustrating the effectiveness of ozonation in removing those available THS sources. Subsequent ozonation and ventilation further reduced the airborne nicotine level to 19 ± 3 ng m^{-3} , which is very close to the average carpet background level.

VOCs in Room Air. Results shown in Figure 4b and Table S2 present the total VOC (TVOC) concentration measured in the chamber during the experiment, corresponding to 56 different compounds. From these, 44 VOCs were quantified by GC/MS, and 12 carbonyls were sampled using DNPH

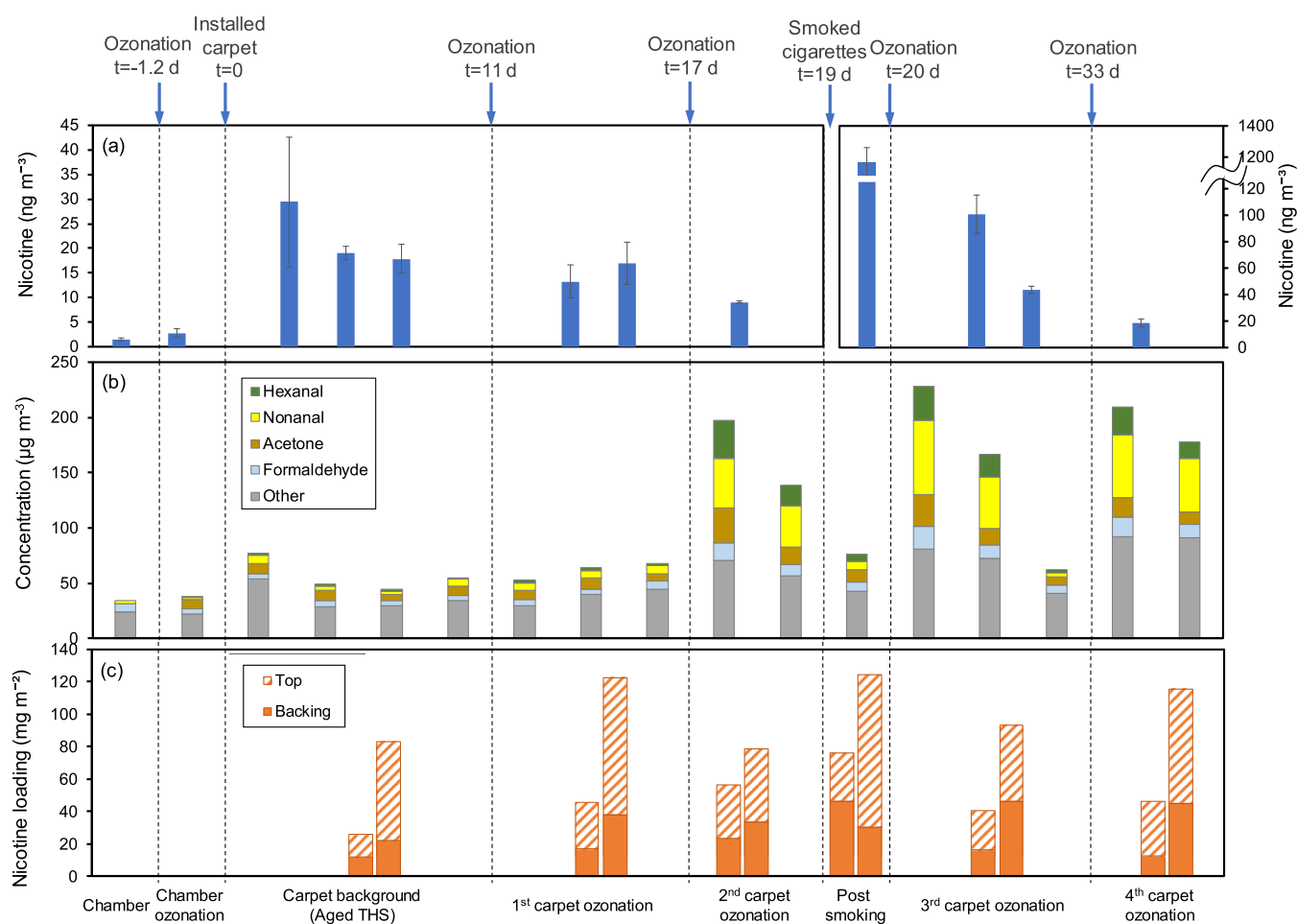


Figure 4. Measurements carried out during the room-sized chamber ozonation experiment. (a) Airborne nicotine concentration; (b) total VOC concentration in room air; (c) carpet-embedded nicotine loading.

cartridges and analyzed by high performance liquid chromatography (HPLC). Background levels associated with laboratory and chamber sources resulted in a TVOC concentration of $34 \mu\text{g m}^{-3}$, and it did not increase significantly due to ozonation of the chamber before the carpet was introduced. Upon installation of the carpet, measurements performed during the 10 d carpet background period showed an average increase in TVOC of 45% with respect to the chamber blank. In the presence of carpet, there was a larger contribution of hexanal and nonanal with respect to chamber blank measurements. The first (low-dose) carpet ozonation did not result in a major increment of TVOCs, but subsequent treatments at higher doses (2nd, 3rd, and 4th carpet ozonation) contributed to a major increase in TVOC levels, driven primarily by increasing nonanal, hexanal, acetone, and formaldehyde concentrations. For the analysis of aldehyde emissions from ozone-treated carpet, these three high-dose ozonation events can be considered a triplicate determination. In each of them, an initial VOC sample was collected approximately 6 h after ozonation ended, once the chamber ozone concentration had dropped to background levels. The predicted aldehyde emission rates at that time, reported in Table S6, were comparable to values reported in the literature for secondary emissions released by carpets exposed to ozone.^{12,14,17,18} A second VOC sample collected approximately 15 h after ozonation showed a concentration ratio with respect to the first VOC sample that was, on average, $C_2/C_1 = 0.78 \pm 0.09$ for

nonanal, 0.59 ± 0.06 for hexanal, 0.36 ± 0.02 for acetone, and 0.48 ± 0.04 for formaldehyde (Figure S10). These values are substantially higher than the expected ratio for a nonsorptive tracer removed by ventilation ($C_2/C_1 = 0.05$) and illustrate how carpet becomes a secondary source of aldehydes desorbing over many hours postozonation. In the case of the very volatile acetone and formaldehyde, the high C_2/C_1 ratios may also be due to their formation as ozonation byproducts in relatively slow surface reactions. The formation of carbonyls in the ozonation of carpet has been attributed to reaction with carpet fibers, coatings, and semivolatile compounds emitted by carpet, all of which evolve as carpet ages.^{16,18–20} In the context of our study, these reactions—along with the formation of other nonvolatile carpet oxidation products described above—illustrate the role of carpet as a chemical barrier protecting THS contaminants present in deep pockets within the material, which are sheltered from the action of ozone and other oxidants.

Carpet-Embedded Nicotine. Results shown in Figure 4c and Table S3 present the surface loading of nicotine in specimens collected from the carpet during the ozonation experiment. In each period, specimens were retrieved from two different areas of the carpet, marked as X and Y and comprising both carpet top and backing. Results show a consistently higher nicotine loading in specimens from the Y area with respect to the X area, despite their relative proximity, illustrating the challenges in quantifying nicotine contami-

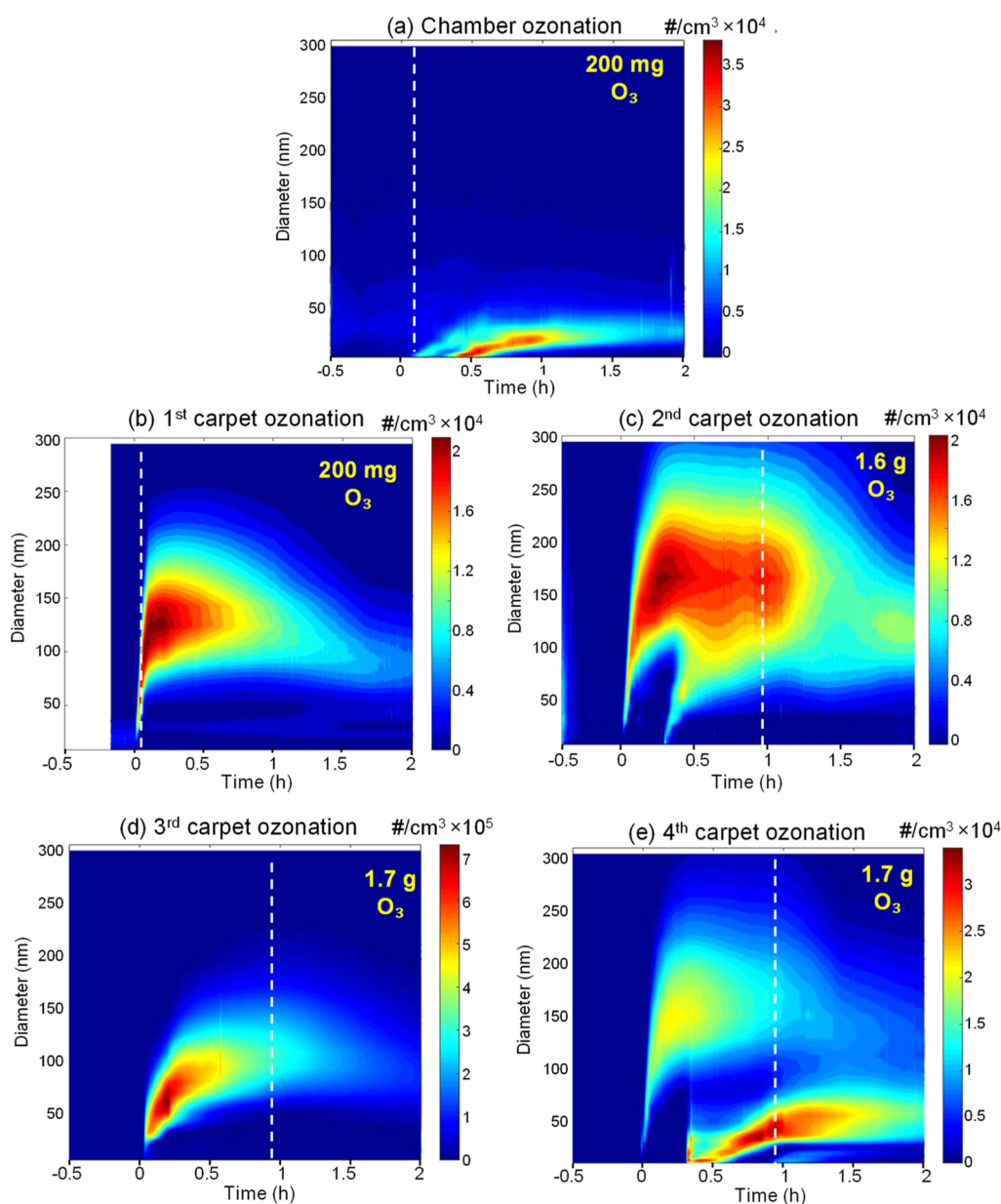


Figure 5. Particle number (PN) concentration and size distribution for (a) background chamber ozonation; (b) 1st carpet ozonation; (c) 2nd carpet ozonation; (d) 3rd carpet ozonation; and (e) 4th carpet ozonation. In each plot, the ozone generator was turned on at $t = 0$ and turned off at the time indicated with the white vertical dotted line. The amount of ozone delivered in each case is indicated in the upper right corner.

nation in these materials. Similarly, nicotine was present in both carpet top and backing materials in relatively comparable proportions. Despite these challenges, the results illustrate clearly that there was no significant depletion of nicotine from the carpet during all of the ozonation periods, illustrating how the carpet sheltered nicotine from oxidation. We anticipate that a similar protective effect could take place with other THS contaminants present alongside nicotine in deep carpet reservoirs. Surface-bound nicotine loading did not increase significantly after smoking the cigarettes owing to the relatively small contribution of new nicotine (estimated to be equal to or less than 1.4 mg m^{-2}) with respect to the amount already present in the carpet.

Particle Emissions. Aerosol particles were formed during ozonation by nucleation and aggregation of oxidized semi-volatile species, as demonstrated by previous studies.^{11,22,36} Figure 5 illustrates the formation and evolution of particulate

number (PN) concentration in the chamber for each ozonation event. In addition, Figure S11 presents the corresponding peak particle mass (PM) concentration calculated in each case. Figure 5a shows a relatively low level of particles of small size ($<50 \text{ nm}$) produced during preliminary ozonation of the chamber, prior to installation of the THS-contaminated carpet. The main particle burst took place at $t = 0.4 \text{ h}$, roughly 15 min after the ozone generator was turned off. This delayed response is consistent with our previous observations in the same chamber.²²

Once the carpet was installed, the first ozonation event produced a different particle burst, illustrated in Figure 5b, taking place immediately as the ozone was generated and with rapid particle growth leading to sizes $>100 \text{ nm}$ in most cases. In this ozonation event, peak PM concentration was 1 order of magnitude higher than that produced in the absence of carpet under similar ozonation conditions ($162 \text{ vs } 18 \text{ } \mu\text{g m}^{-3}$),

suggesting that ozone reaction with carpet fibers and with THS compounds present in the carpet is a strong source of particulate matter. The second ozonation event (Figure 5c) produced a bimodal generation burst, with an initial rapid growth leading to larger particle sizes than those produced by the first ozonation, followed by a relatively smaller burst of smaller particles (<50 nm) at $t = 0.4$ h. The peak PM concentration was $387 \mu\text{g m}^{-3}$.

After cigarettes were smoked in the chamber, a new ozonation event led to the formation of even higher aerosol PN concentrations, as shown in Figure 5d, with a rapid burst of relatively small particles (<100 nm). The corresponding peak PM was $1467 \mu\text{g m}^{-3}$, the highest recorded, due to the presence of freshly deposited THS sources on all chamber surfaces. The aerosol emission patterns changed significantly in the second ozonation (Figure 5e), with much lower emission rates in a bimodal burst pattern in which the highest PN concentration was in small size particles <50 nm. In this final ozonation event, the recorded peak PM concentration ($290 \mu\text{g m}^{-3}$) was comparable to those from previous carpet ozonation events.

Implications for Indoor Environmental Quality. This study has illustrated the role of the wall-to-wall carpeting commonly found in US dwellings as deep reservoirs that accumulate THS, becoming a secondary source that releases tobacco contaminants for a long time after smoking has ended. The magnitude of that secondary source can be estimated from the measurements reported here by calculating the emission rate observed in our room-sized experiment as

$$E = \frac{\lambda \times V \times (C - C_0)}{A} \quad (5)$$

where λ is the chamber AER, V the chamber volume, C the average airborne nicotine concentration with the carpet installed, C_0 the chamber background nicotine concentration before installing the carpet, and A the carpet area. In our study, we determined an emission rate $E = 950 \text{ ng day}^{-1} \text{ m}^{-2}$. Hence, in a contaminated home with 50–100 m^2 of carpet, this THS source could amount to a nicotine release of 47–95 $\mu\text{g day}^{-1}$. This amount represents a non-negligible fraction of the nicotine emitted by one cigarette during smoking, as shown in Table S7. Since carpet is not the only reservoir/secondary source in THS-contaminated homes and the carpet used here (from home A) represents a typical rather than a worst-case scenario, it is possible that daily nicotine re-emissions from deep reservoirs in heavily contaminated homes can become comparable with the amount released by one cigarette during smoking. In homes where active smoking takes place, nonsmokers' exposures associated with THS emissions may not represent the main contribution to the total burden of harm associated with tobacco use compared with inhalation of secondhand smoke. This is particularly true when a large number of cigarettes are smoked indoors (e.g., one pack per day) in the presence of nonsmokers. However, surveys of smokers' homes with children showed that at least half of them implement complete smoking bans, and the average number of cigarettes smoked indoors with a child present is typically less than one pack per week.^{3,37,38} In such scenarios, THS may be a major source of exposure to tobacco smoke pollutants in children. High THS concentrations have been reported in surfaces, dust, and indoor air in environments without active smoking, such as homes of former smokers^{27,39} and those implementing voluntary indoor smoking bans.³ It is in those

cases where the contribution of THS to occupants' exposure and health outcomes is most relevant. The same is true for other settings where emissions from THS embedded in building materials can be significant, such as hotel rooms⁴⁰ and short-term rentals.

Deep reservoirs are effective in protecting THS contaminants from reaction with ozone, even when ozone is released at very high concentrations for the purpose of remediation. The effect of ozonation is not the same on every THS compound. While this study has only explored its reaction with nicotine and PAHs, our results suggest that significant differences can be found among different chemical functionalities. Nicotine is very relevant as a THS tracer and as a precursor of carcinogenic tobacco-specific nitrosamines.^{41,42} Ozonation did not prove effective in removing nicotine, particularly in aged carpets where most of the compound was likely stored in deep reservoirs. These results also suggest that nicotine and other THS compounds are not only sheltered during remediation treatment but also protected from long-term degradation by reaction with low levels of ozone and other oxidants naturally present in indoor air. Ozone and other reactive species are expected to be present in higher concentrations in naturally ventilated buildings (e.g., by opening windows) and can be significantly reduced in mechanical ventilation ductwork and filter banks.¹⁰ The protective mechanism may involve the reaction of incoming ozone with the carpet matrix, developing a reactive diffusional layer in which ozone is partially or fully depleted before it can reach the THS absorbed in deep small pores inside the fibers. The carpet matrix includes not only fibers and other carpet constituents (e.g., dyes and fluorinated coatings) but also adventitious organic films and skin oils, which contribute to scavenging ozone.⁴³ A similar mechanism was described in the evaluation of color fastness in nylon carpet fibers exposed to high levels of ozone, showing an initial fading due to reaction of the most accessible surface dye, followed by slower color change rates as ozone is scavenged before penetrating into the filament and reaching the remaining dye.⁴⁴ This effect was further illustrated by a recent study using computational fluid dynamics simulation, which described significant ozone concentration gradients resulting in reduced mass transport within the carpet surface boundary layer.⁴⁵ In addition to ozone scavenging, the ozonation efficiency of semivolatile species trapped in deep pores is also limited by the slow diffusion of these compounds out of these reservoirs, comparable to the depletion of ozone reactive material accumulated in HVAC filters.⁴⁶ Considering the results obtained with PAHs, both aged and fresh THS samples exhibited significant elimination of these compounds, suggesting that ozonation may be an effective treatment for at least a subset of THS contaminants. The fact that PAHs have a very low volatility may result in lower penetration within the carpet matrix, remaining more exposed to incoming ozone.

■ ASSOCIATED CONTENT

Supporting Information

The Supporting Information is available free of charge at <https://pubs.acs.org/doi/10.1021/acs.est.3c01628>.

Description of measurements performed in smokers' homes; characterization of carpet samples; description of laboratory experimental setups and methods; analytical methods for nicotine, PAHs, VOCs, volatile carbonyls,

aerosol particles, and high-resolution mass spectrometric analyses; ATR-FTIR spectra of carpets, ozone concentration traces, and consumption rates; loading of PAHs in carpet and removal efficiency; results from ESI-MS and CIMS analyses; results from room-sized chamber experiments (ozone concentration, emission rates of carbonyls, and peak particle mass concentration); and predicted nicotine emission rates (PDF)

AUTHOR INFORMATION

Corresponding Authors

Xiaochen Tang – *Indoor Environment Group, Lawrence Berkeley National Laboratory, Berkeley, California 94720, United States*; Email: XTang@lbl.gov

Hugo Destailats – *Indoor Environment Group, Lawrence Berkeley National Laboratory, Berkeley, California 94720, United States*; orcid.org/0000-0002-2132-3816; Email: HDestailats@lbl.gov

Authors

Clément Gambier – *Indoor Environment Group, Lawrence Berkeley National Laboratory, Berkeley, California 94720, United States*

Nicolás López-Gálvez – *School of Public Health, San Diego State University, San Diego, California 92182, United States*

Samuel Padilla – *School of Public Health, San Diego State University, San Diego, California 92182, United States*; Present Address: San Diego State University Research Foundation, San Diego, CA 92182

Vi H. Rapp – *Indoor Environment Group, Lawrence Berkeley National Laboratory, Berkeley, California 94720, United States*

Marion L. Russell – *Indoor Environment Group, Lawrence Berkeley National Laboratory, Berkeley, California 94720, United States*

Liana M. Klivansky – *Molecular Foundry, Lawrence Berkeley National Laboratory, Berkeley, California 94720, United States*

Raphael Mayorga – *Department of Chemistry, University of California Riverside, Riverside, California 92521, United States*

Charles Perrino – *School of Public Health, University of California Berkeley, Berkeley, California 94720, United States*

Lara A. Gundel – *Indoor Environment Group, Lawrence Berkeley National Laboratory, Berkeley, California 94720, United States*

Eunha Hoh – *School of Public Health, San Diego State University, San Diego, California 92182, United States*; orcid.org/0000-0002-4075-040X

Nathan G. Dodder – *School of Public Health, San Diego State University, San Diego, California 92182, United States*; orcid.org/0000-0001-5913-1767

S. Katharine Hammond – *School of Public Health, University of California Berkeley, Berkeley, California 94720, United States*

Haofei Zhang – *Department of Chemistry, University of California Riverside, Riverside, California 92521, United States*; orcid.org/0000-0002-7936-4493

George E. Matt – *Department of Psychology, San Diego State University, San Diego, California 92182, United States*; orcid.org/0000-0001-5604-4609

Penelope J. E. Quintana – *School of Public Health, San Diego State University, San Diego, California 92182, United States*

Complete contact information is available at: <https://pubs.acs.org/10.1021/acs.est.3c01628>

Notes

The authors declare no competing financial interest.

ACKNOWLEDGMENTS

This study was supported by the University of California's TRDRP THS Consortium grants 28PT-0075 (Destailats), T32PT5965 (Destailats) and 28PT-0079 (Quintana). The Lawrence Berkeley National Laboratory operates under the U.S. Department of Energy contract DE-AC02-05CH11231. Work at the Molecular Foundry was supported by the Office of Science, Office of Basic Energy Sciences, of the U.S. Department of Energy under Contract no. DE-AC02-05CH11231. We thank Sharon Chen (LBNL) for her support in aerosol particle measurements.

REFERENCES

- (1) Jacob, P.; Benowitz, N.; Destailats, H.; Gundel, L. A.; Hang, B.; Martins-Green, M.; Matt, G. E.; Quintana, P. J. E.; Samet, J.; Schick, S.; Talbot, P.; Aquilina, N. J.; Hovell, M. F.; Mao, J.-H.; Whitehead, T. P. Thirdhand smoke: New evidence, challenges and future directions. *Chem. Res. Toxicol.* **2017**, *30*, 270–294.
- (2) Matt, G. E.; Quintana, P. J. E.; Destailats, H.; Gundel, L. A.; Sleiman, M.; Singer, B. C.; Jacob, P.; Benowitz, N.; Winickoff, J. P.; Rehan, V.; Talbot, P.; Schick, S.; Samet, J.; Wang, Y.; Hang, B.; Martins-Green, M.; Pankow, J. F.; Hovell, M. F. Thirdhand tobacco smoke: Emerging evidence and arguments for a multidisciplinary research agenda. *Environ. Health Perspect.* **2011**, *119*, 1218–1226.
- (3) Matt, G. E.; Quintana, P. J. E.; Hoh, E.; Zakarian, J. M.; Dodder, N. G.; Record, R. A.; Hovell, M. F.; Mahabee-Gittens, E. M.; Padilla, S.; Markman, L.; Watanabe, K.; Novotny, T. E. Persistent tobacco smoke residue in multiunit housing: Legacy of permissive indoor smoking policies and challenges in the implementation of smoking bans. *Prev. Med. Rep.* **2020**, *18*, 101088.
- (4) Matt, G. E.; Quintana, P. J. E.; Hoh, E.; Zakarian, J. M.; Dodder, N. G.; Record, R. A.; Hovell, M. F.; Mahabee-Gittens, E. M.; Padilla, S.; Markman, L.; Watanabe, K.; Novotny, T. E. Remediating thirdhand smoke pollution in multiunit housing: Temporary reductions and the challenges of persistent reservoirs. *Nicotine Tob. Res.* **2021**, *23*, 364–372.
- (5) Singer, B. C.; Hodgson, A. T.; Guevarra, K. S.; Hawley, E. L.; Nazaroff, W. W. Gas-phase organics in environmental tobacco smoke. 1. Effects of smoking rate, ventilation and furnishing level on emission factors. *Environ. Sci. Technol.* **2002**, *36*, 846–853.
- (6) Singer, B. C.; Hodgson, A. T.; Nazaroff, W. W. Gas-phase organics in environmental tobacco smoke: 2. Exposure-relevant emission factors and indirect exposures from habitual smoking. *Atmos. Environ.* **2003**, *37*, 5551–5561.
- (7) Tang, X.; Benowitz, N.; Gundel, L. A.; Hang, B.; Havel, C. M.; Hoh, E.; Jacob, P., III; Mao, J.-H.; Martins-Green, M.; Matt, G. E.; Quintana, P. J. E.; Russell, M. L.; Sarker, A.; Schick, S. F.; Snijders, A. M.; Destailats, H. Thirdhand exposures to tobacco-specific nitrosamines through inhalation, dust ingestion, dermal uptake, and epidermal chemistry. *Environ. Sci. Technol.* **2022**, *56*, 12506–12516.
- (8) Poppendieck, D.; Hubbard, H.; Ward, M.; Weschler, C.; Corsi, R. L. Ozone reactions with indoor materials during building disinfection. *Atmos. Environ.* **2007**, *41*, 3166–3176.
- (9) Zakarian, J. M.; Quintana, P. J. E.; Winston, C.; Matt, G. E. Hotel smoking policies and their implementation: a survey of California hotel managers. *Tob. Induced Dis.* **2017**, *15*, 40.
- (10) Nazaroff, W. W.; Weschler, C. J. Indoor ozone: Concentrations and influencing factors. *Indoor Air* **2022**, *32*, No. e12942.

- (11) Sleiman, M.; Destailhats, H.; Smith, J. D.; Liu, C.-L.; Ahmed, M.; Wilson, K. R.; Gundel, L. A. Secondary organic aerosol formation from ozone-initiated reactions with nicotine and secondhand tobacco smoke. *Atmos. Environ.* **2010**, *44*, 4191–4198.
- (12) Abbass, O. A.; Sailor, D. J.; Gall, E. T. Effect of fiber material on ozone removal and carbonyl production from carpets. *Atmos. Environ.* **2017**, *148*, 42–48.
- (13) Coleman, B. K.; Destailhats, H.; Hodgson, A. T.; Nazaroff, W. W. Ozone consumption and volatile byproduct formation from surface reactions with aircraft cabin materials and clothing fabrics. *Atmos. Environ.* **2008**, *42*, 642–654.
- (14) Gall, E.; Darling, E.; Siegel, J. A.; Morrison, G. C.; Corsi, R. L. Evaluation of three common green building materials for ozone removal, and primary and secondary emissions of aldehydes. *Atmos. Environ.* **2013**, *77*, 910–918.
- (15) Morrison, G. C.; Nazaroff, W. W. The rate of ozone uptake on carpets: Experimental studies. *Environ. Sci. Technol.* **2000**, *34*, 4963–4968.
- (16) Morrison, G. C.; Nazaroff, W. W. Ozone interactions with carpet: Secondary emissions of aldehydes. *Environ. Sci. Technol.* **2002**, *36*, 2185–2192.
- (17) Nicolas, M.; Ramalho, O.; Maupetit, F. Reactions between ozone and building products: Impact on primary and secondary emissions. *Atmos. Environ.* **2007**, *41*, 3129–3138.
- (18) Wang, H.; Morrison, G. C. Ozone-initiated secondary emission rates of aldehydes from indoor surfaces in four homes. *Environ. Sci. Technol.* **2006**, *40*, S263–S268.
- (19) Wang, H.; Morrison, G. C. Ozone-surface reactions in five homes: Surface reaction probabilities, aldehyde yields, and trends. *Indoor Air* **2010**, *20*, 224–234.
- (20) Weschler, C. J.; Hodgson, A. T.; Wooley, J. D. Indoor chemistry: Ozone, volatile organic compounds, and carpets. *Environ. Sci. Technol.* **1992**, *26*, 2371–2377.
- (21) Lee, M.; Lee, M. S.; Wakida, T.; Tokuyama, T.; Inoue, G.; Ishida, S.; Itazu, T.; Miyaji, Y. Chemical modification of Nylon 6 and polyester fabrics by ozone-gas treatment. *J. Appl. Polym. Sci.* **2006**, *100*, 1344–1348.
- (22) Tang, X.; Ramirez-González, N.; Russell, M. L.; Maddalena, R. L.; Gundel, L. A.; Destailhats, H. Chemical changes in thirdhand smoke associated with remediation using an ozone generator. *Environ. Res.* **2021**, *198*, 110462.
- (23) Haines, S. R.; Adams, R. I.; Boor, B. E.; Bruton, T. A.; Downey, J.; Ferro, A. R.; Gall, E.; Green, B. J.; Hegarty, B.; Horner, E.; Jacobs, D. E.; Lemieux, P.; Misztal, P. K.; Morrison, G. C.; Perzanowski, M.; Reponen, T.; Rush, R. E.; Virgo, T.; Alkhatyri, C.; Bope, A.; Cochran, S.; Cox, J.; Donohue, A.; May, A. A.; Nastasi, N.; Nishioka, M.; Renninger, N.; Tian, Y.; Uebel-Niemeier, C.; Wilkinson, D.; Wu, T.; Zambrana, J.; Dannemiller, K. C. Ten questions concerning the implications of carpet on indoor chemistry and microbiology. *Build. Environ.* **2020**, *170*, 106589.
- (24) Quintana, P. J. E., Reducing exposure to thirdhand smoke in multiunit housing, 2019. http://trdrp.yes4yes.com/fundedresearch/grant_page.php?grant_id=51063 (accessed Feb 16, 2023).
- (25) Quintana, P. J. E.; Matt, G. E.; Chatfield, D.; Zakarian, J. M.; Fortmann, A. L.; Hoh, E. Wipe sampling for nicotine as a marker of thirdhand tobacco smoke contamination on surfaces in homes, cars and hotels. *Nicotine Tob. Res.* **2013**, *15*, 1555–1563.
- (26) Matt, G. E.; Quintana, P. J. E.; Hoh, E.; Zakarian, J. M.; Chowdhury, Z.; Hovell, M. F.; Jacob, P., III.; Watanabe, K.; Theweny, T. S.; Flores, V.; Nguyen, A.; Dhaliwal, N.; Hayward, G. A casino goes smoke free: A longitudinal study of secondhand and thirdhand smoke pollution and exposure. *Tobac. Control* **2018**, *27*, 643–649.
- (27) Matt, G. E.; Quintana, P. J. E.; Zakarian, J. M.; Fortmann, A. L.; Chatfield, D.; Hoh, E.; Uribe, A. M.; Hovell, M. F. When smokers move out and non-smokers move in: residential thirdhand smoke pollution and exposure. *Tobac. Control* **2011**, *20*, No. e1.
- (28) Hammond, S. K.; Leaderer, B. P.; Roche, A. C.; Schenker, M. Collection and analysis of nicotine as a marker for environmental tobacco smoke. *Atmos. Environ.* **1987**, *21*, 457–462.
- (29) Holland-Moritz, K.; Siesler, H. W. Infrared spectroscopy of polymers. *Appl. Spectrosc. Rev.* **1976**, *11*, 1–55.
- (30) Rim, D.; Gall, E. T.; Maddalena, R. L.; Nazaroff, W. W. Ozone reaction with interior building materials: Influence of diurnal ozone variation, temperature and humidity. *Atmos. Environ.* **2016**, *125*, 15–23.
- (31) DellaValle, C. T.; Deziel, N. C.; Jones, R. R.; Colt, J. S.; DeRoos, A. J.; Cerhan, J. R.; Cozen, W.; Severson, R. K.; Flory, A. R.; Morton, L. M.; Ward, M. H. Polycyclic aromatic hydrocarbons: determinants of residential carpet dust levels and risk of non-Hodgkin lymphoma. *Cancer, Causes Control* **2016**, *27*, 1–13.
- (32) Lewis, R. G.; Fortune, C. R.; Willis, R. D.; Camann, D. E.; Antley, J. T. Distribution of pesticides and polycyclic aromatic hydrocarbons in house dust as a function of particle size. *Environ. Health Perspect.* **1999**, *107*, 721–726.
- (33) Hoh, E.; Hunt, R. N.; Quintana, P. J. E.; Zakarian, J. M.; Chatfield, D.; Wittry, B. C.; Rodriguez, E.; Matt, G. E. Environmental tobacco smoke as a source of polycyclic aromatic hydrocarbons in settled household dust. *Environ. Sci. Technol.* **2012**, *46*, 4174–4183.
- (34) Yu, C. H.; Yiin, L.-M.; Tina Fan, Z. H.; Rhoads, G. G. Evaluation of HEPA vacuum cleaning and dry steam cleaning in reducing levels of polycyclic aromatic hydrocarbons and house dust mite allergens in carpets. *J. Environ. Monit.* **2009**, *11*, 205–211.
- (35) Keyte, I. J.; Harrison, R. M.; Lammel, G. Chemical reactivity and long-range transport potential of polycyclic aromatic hydrocarbons - A review. *Chem. Soc. Rev.* **2013**, *42*, 9333–9391.
- (36) Wang, C.; Collins, D. B.; Hems, R. F.; Borduas, N.; Antinolo, M.; Abbatt, J. P. D. Exploring Conditions for Ultrafine Particle Formation from Oxidation of Cigarette Smoke in Indoor Environments. *Environ. Sci. Technol.* **2018**, *52*, 4623–4631.
- (37) Matt, G. E.; Merianos, A. L.; Quintana, P. J. E.; Hoh, E.; Dodder, N. G.; Mahabee-Gittens, E. M. Prevalence and income-related disparities in thirdhand smoke exposure to children. *JAMA Netw. Open* **2022**, *5*, No. e2147184.
- (38) Mahabee-Gittens, E. M.; Matt, G. E.; Jandarov, R. A.; Merianos, A. L. The associations of trans-3'-hydroxy cotinine, cotinine, and the nicotine metabolite ratio in pediatric patients with tobacco smoke exposure. *Int. J. Environ. Res. Public Health* **2023**, *20*, 5639.
- (39) Matt, G. E.; Quintana, P. J. E.; Zakarian, J. M.; Hoh, E.; Hovell, M. F.; Mahabee-Gittens, M.; Watanabe, K.; Datuin, K.; Vue, C.; Chatfield, D. When smokers quit: exposure to nicotine and carcinogens persists from thirdhand smoke pollution. *Tobac. Control* **2016**, *26*, 548–556.
- (40) Matt, G. E.; Quintana, P. J. E.; Fortmann, A. L.; Zakarian, J. M.; Galaviz, V. E.; Chatfield, D.; Hoh, E.; Hovell, M. F.; Winston, C. Thirdhand smoke and exposure in California hotels: non-smoking rooms fail to protect non-smoking hotel guests from tobacco smoke exposure. *Tobac. Control* **2014**, *23*, 264–272.
- (41) Sleiman, M.; Gundel, L. A.; Pankow, J. F.; Jacob, P., III.; Singer, B. C.; Destailhats, H. Formation of carcinogens indoors by surface-mediated reactions of nicotine with nitrous acid, leading to potential thirdhand smoke hazards. *Proc. Natl. Acad. Sci. U.S.A.* **2010**, *107*, 6576–6581.
- (42) Sleiman, M.; Maddalena, R. L.; Gundel, L. A.; Destailhats, H. Rapid and sensitive gas chromatography-ion-trap tandem mass spectrometry method for the determination of tobacco-specific N-nitrosamines in secondhand smoke. *J. Chromatogr. A* **2009**, *1216*, 7899–7905.
- (43) Ault, A. P.; Grassian, V. H.; Carslaw, N.; Collins, D. B.; Destailhats, H.; Donaldson, D. J.; Farmer, D. K.; Jimenez, J. L.; McNeill, V. F.; Morrison, G. C.; O'Brien, R. E.; Shiraiwa, M.; Vance, M. E.; Wells, J. R.; Xiong, W. Indoor surface chemistry: Developing a molecular picture of reactions on indoor interfaces. *Chem* **2020**, *6*, 3203–3218.
- (44) Motamedian, F.; Broadbent, A. D. Effects of dye distribution in Nylon filament yarns on the dyeing color yield and fastness properties. *Ind. Eng. Chem. Res.* **1999**, *38*, 4656–4662.

(45) Pei, G.; Xuan, Y.; Morrison, G. C.; Rim, D. Understanding ozone transport and deposition within indoor surface boundary layers. *Environ. Sci. Technol.* **2022**, *56*, 7820–7829.

(46) Zhao, P.; Siegel, J. A.; Corsi, R. L. Ozone removal by HVAC filters. *Atmos. Environ.* **2007**, *41*, 3151–3160.

Recommended by ACS

Occurrence of 1,3-Diphenylguanidine, 1,3-Di-*o*-tolylguanidine, and 1,2,3-Triphenylguanidine in Indoor Dust from 11 Countries: Implications for Human Exposure

Zhong-Min Li and Kurunthachalam Kannan

APRIL 03, 2023

ENVIRONMENTAL SCIENCE & TECHNOLOGY

[READ](#) 

Insights into Health Risks of Face Paint Application to Opera Performers: The Release of Heavy Metals and Stage-Light-Induced Production of Reactive Oxygen Species

Bin Wang, Rong Ji, *et al.*

FEBRUARY 23, 2023

ENVIRONMENTAL SCIENCE & TECHNOLOGY

[READ](#) 

Bleach Emissions Interact Substantially with Surgical and KN95 Mask Surfaces

Nirvan Bhattacharyya, Lea Hildebrandt Ruiz, *et al.*

APRIL 16, 2023

ENVIRONMENTAL SCIENCE & TECHNOLOGY

[READ](#) 

Increased JUUL Emissions from Initial Puffs after Removing and Reinserting Pod

Eric K. Soule, Jack Pender, *et al.*

MARCH 08, 2022

CHEMICAL RESEARCH IN TOXICOLOGY

[READ](#) 

[Get More Suggestions >](#)

SUPPORTING INFORMATION

Remediation of thirdhand tobacco smoke with ozone: Probing deep reservoirs in carpets

Xiaochen Tang^{1,*}, Clément Gambier¹, Nicolas Lopez-Galvez², Samuel Padilla², Vi H. Rapp¹,
Marion L. Russell¹, Liana M. Klivansky³, Raphael Mayorga⁴, Charles Perrino⁵, Lara A. Gundel¹,
Eunha Hoh², Nathan G. Dodder², S. Katharine Hammond⁵, Haofei Zhang⁴, Georg Matt⁶,
Penelope J. E. Quintana², Hugo Destailats^{1,*}

1. *Indoor Environment Group, Lawrence Berkeley National Laboratory, Berkeley, California 94720, United States*
2. *School of Public Health, San Diego State University, San Diego, California 92182, United States*
3. *Molecular Foundry, Lawrence Berkeley National Laboratory, Berkeley, California, 94720, United States*
4. *Department of Chemistry, University of California Riverside, Riverside, California 92521, United States*
5. *School of Public Health, University of California Berkeley, Berkeley, California 04720, United States*
6. *Department of Psychology, San Diego State University, San Diego, California 92182, United States*

* Corresponding author E-mail: XTang@lbl.gov and HDestailats@lbl.gov

Summary: 27 pages, 11 figures, 7 tables, 6 sections

TABLE OF CONTENTS

SECTION, FIGURE, TABLE	PAGE
Section S1. Measurements performed in smokers' homes (San Diego)	S3
Section S2. Characterization of carpet samples	S4
Table S1. Environmental, physical and chemical properties of field carpet samples	S5

Figure S1. Photos illustrating tested carpet specimens	S6
Figure S2. Chamber for exposing clean carpet specimens to fresh THS	S7
Section S3. Determination of air exchange rate (AER)	S7
Figure S3. Schematic of bench-scale chamber experimental setup for ozonation	S8
Figure S4. Carpet specimen handling	S8
Section S4. Determination of nicotine and PAH loading in carpet	S9
Section S5. Analysis of carpet-embedded chemicals using high resolution instruments	S10
Table S2. Room-size chamber experiment timeline, nicotine TVOC concentration	S11
Table S3. Room-size chamber experiment timeline, carpet-bound nicotine loading	S12
Section S6. Measurement of gas phase species and aerosols in room-sized chamber	S13
Figure S5. ATR-FTIR spectra	S15
Figure S6. Ozone concentration in bench-scale experiments	S16
Figure S7. Ozone consumption rate as a function of nicotine loading	S17
Table S4. PAH loading in carpet specimens and removal efficiency after ozonation	S18
Figure S8. Loading of Benzo[a]pyrene measured in different carpet samples	S19
Table S5. Results from ESI-MS and CIMS analysis	S20
Figure S9. Ozone concentration during five room-sized chamber ozonation experiments	S21
Table S6. Emission rates of carbonyls in the room-size chamber ozonation experiment	S22
Figure S10. Ratio between aldehyde concentration measured in the second and first VOC sample, for each of the high-dose carpet ozonation tests.	S22
Figure S11. Peak particle mass concentration ($\mu\text{g m}^{-3}$) calculated for each ozonation experiment from FMPS measurement	S23
Table S7. Nicotine emission rates predicted from our room-sized chamber, and reported in the literature	S24
References	S25

Section S1. Measurements performed in smokers' homes (San Diego)

HH5 study selection process. A total of 54 homes were screened by measuring the nicotine surface levels of doors, walls, and built-in cabinets. The average nicotine surface loading was calculated, and homes with levels above $10 \mu\text{g m}^{-2}$ were selected for additional sampling, which included collection of THS contaminated carpet samples. In four of the selected homes, about 5 – 6 m^2 of the top carpet layer and backing padding (when present) were removed and shipped to LBNL for further studies.

Nicotine on surfaces and in dust. Prescreened cotton rounds were wetted with 1.5 mL water containing 0.1% ascorbic acid, and used to wipe over a 100 cm^2 surface area of a selected hard indoor surface (e.g. door, wall, cabinet). House dust samples were collected in a Teflon bottle from each selected home, from a 1-m^2 area using a high-volume-small surface-sampler cyclone vacuum (HVS4, CS3, Venice, FL, USA). All samples were stored at -20°C prior to analysis in the Environmental Health Laboratory at San Diego State University. Dust and wipe samples were spiked, extracted with a QueChERs technique in acetonitrile and analyzed by isotope-dilution liquid chromatography-tandem mass spectrometry (LC-MS/MS) using electrospray ionisation (ESI) on a Thermo-Finnigan TSQ Quantum Mass Spectrometer. Analytic methods have been reported in more detail elsewhere [1, 2].

Nicotine in room air. Airborne nicotine was collected in side-by-side triplicate determinations onto bisulfate-coated Teflon filters. The sampling flow rate of 2 to 4 L min^{-1} was maintained for 48 h. After collection, filter samples were stored in a freezer and sent to LBNL in a cooled container. The mass of nicotine collected in each sample was determined at UC Berkeley by extracting each filter with a solution of 95% water and 5% methanol, and GC/MS analysis, as described below in Section S6 (Hammond method). The range of nicotine standard concentration was $0.01 \mu\text{g mL}^{-1}$ to $10 \mu\text{g mL}^{-1}$ for the GC/MS method calibration.

Section S2. Characterization of carpet samples

Physical characterization. Fiber volume was calculated by measuring the width and length of individual strand of carpet fiber, then taking it as a cylinder to calculate its volume. Carpets from homes A and C were cut (twist) pile, and those from homes B and D were loop pile. Therefore, the calculated fiber volume of the carpets was low for A and C (35-36 mm³) and higher for B and D (257-439 mm³).

FTIR Measurements. The infrared spectra were recorded in a Nicolet iS50 FTIR (Thermo Fisher) collected over the mid-IR region using a KBr beam splitter and a built-in diamond crystal attenuated total reflectance (ATR). The IR spectra were averaged from 32 scans, and the spectral resolution was 4 cm⁻¹. Carpet spectra were obtained by applying the carpet directly on the surface of the ATR crystal. All spectra were blank-subtracted and baseline-corrected using the OMNIC software from Nicolet.

Table S1. Environmental, physical and chemical properties of field carpet samples.

HOME ID		A	B	C	D
Home type		Town house (3-story)	Apartment (1-story)	RV trailer	Apartment (studio)
Central AC		Yes	No	No	No
Smoking history (year)		8	15	6	25
Sampling and carpet retrieval date		1/12/2021	10/11/2021	10/18/2021	4/25/2022
Daily average T (°C)		14	16	17	19
Daily average RH (%)		41	55	65	56
Carpet fiber material	Top	Nylon	Nylon	Nylon	Polypropylene
	Backing	Polyurethane	Polyurethane	N/A	N/A
Carpet fiber cut type		Twist (cut)	Loop	Twist (cut)	Loop
Fiber volume (mm ³)		35	439	36	257
Nicotine concentration in indoor air (µg m ⁻³)		0.24	3.6	0.52	0.37
Nicotine concentration in dust (µg g ⁻¹)		380	439	69	10
Carpet nicotine loading, from the analysis of dust (µg m ⁻²)		858	322	221	13
Nicotine hard surfaces loading, from surface wipes (mg m ⁻²)		0.78	79	0.96	14
Carpet nicotine concentration, from solvent extraction (ng mg ⁻¹)	Top	9.3	30	7.4	<LOQ
	Backing	24	87	NA	NA
Carpet nicotine loading, from solvent extraction (mg m ⁻²)	Top	26	62	17.6	<LOQ
	Backing	23	102	NA	NA

(a) Unused clean carpet top and backing



Top



Backing

(b) Carpet (top and backing) from smoker's homes



Top



Backing

Figure S1. Photos of (a) unused clean carpet top and backing, and (b) top and backing of carpet collected from smoker's homes.

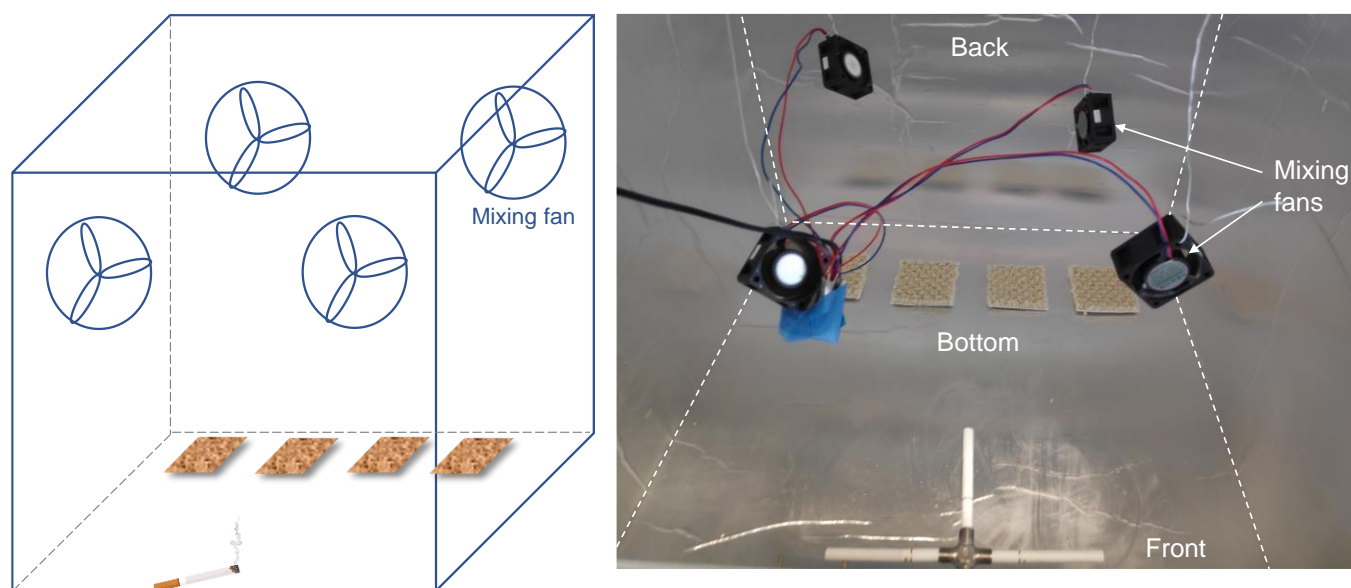


Figure S2. Chamber for exposing clean carpet specimens to fresh THS.

Section S3. Determination of air exchange rate (AER)

150-L smoke exposure chamber. A large amount of CO₂ was injected into the chamber from a cylinder. Within a few minutes, and the real-time CO₂ concentration decay was monitored and recorded with a CO₂ sensor (Aranet4), until levels dropped close to ambient levels (~440 ppm). After subtracting the measured ambient CO₂ level, the curves of CO₂ concentration vs. time were fitted with mono-exponential decay functions.

20-m³ room-sized chamber. A similar method was used to determine the AER in the room-sized chamber in which carpet ozonation tests were performed. Immediately before and at the end of the tests, CO₂ was injected to the room from a cylinder, and the real-time concentration decay was followed with an EGM-4 CO₂ analyzer (PP Systems, Ambury, MA). Given our experience operating this chamber over many years, this number of CO₂ decay measurements was sufficient to determine AER, which does not usually drift nor fluctuate when the chamber is operated under constant conditions. The chamber is nested inside a dedicated air-conditioned building, which minimizes fluctuations due to outdoor temperature swings.

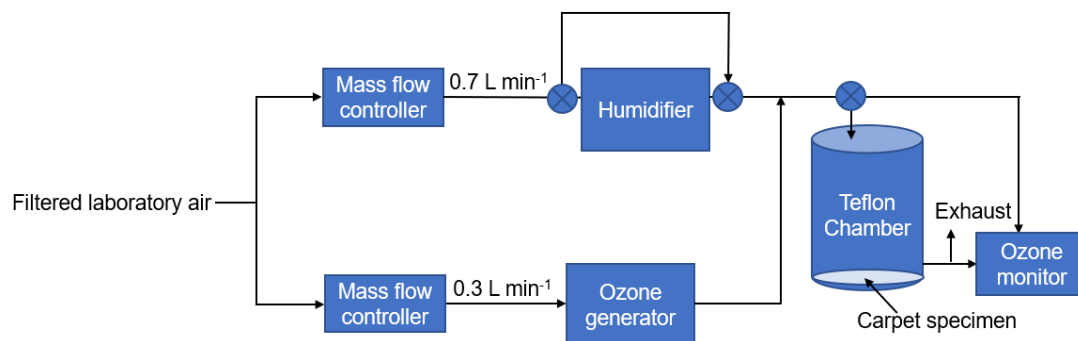


Figure S3. Schematic of bench-scale chamber experimental setup for ozonation

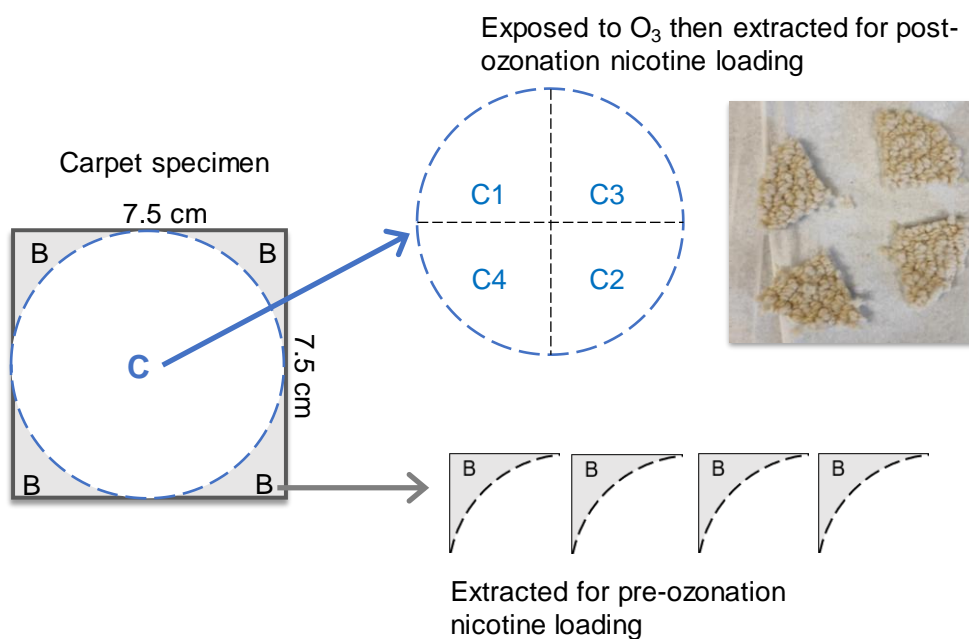


Figure S4. Carpet specimen handling. For each bench-scale chamber experiment, a piece of carpet specimen (7.5 cm by 7.5 cm) was cut to a circle of 7.5 cm diameter (C) to fit in the chamber for ozone exposure, and the remaining corners (B) were used to determine the pre-ozonation nicotine loading on the specimen. After the experiment, the exposed piece was cut into four quarters (C1, C2, C3, C4).

Section S4. Determination of nicotine and PAH loading in carpet

Nicotine. Methanol was used as a solvent to extract nicotine from carpet top and backing. Carpet specimens of known weight were cut into small pieces and put inside glass vials with lids. Known amounts of methanol completely covered each carpet specimen inside the vial, which was placed inside an ultrasonic bath for 30 minutes. At the end of this period, the solvent was transferred to an empty vial and weighed with an analytical balance. The extract was injected into a GC/MS (Agilent 5977), and nicotine concentration was determined in splitless mode, with oven temperature ramping over a range of 30–310 °C. The calibration range was 1-50 ng/μL. In preliminary tests, a second aliquot of clean methanol was added to the vial containing the extracted carpet specimen, and was sonicated for another 30 minutes. The supernatant was removed and injected into GC/MS and analyzed for nicotine concentration. The second extraction contained <10% of the total nicotine, and for that reason only one extraction was used for most sample extractions.

PAHs. An alternative method was implemented, using an accelerated solvent extraction (ASE) system (Dionex ASE 200) with a 1:1 mixture of acetone and hexane (volume ratio). During the extraction, the carpet top specimens were heated by an oven to 50 °C under high pressure (1,500 psi). Two successive extractions were made, and the final volume of extracts was about 15 mL, with 4 mL of which subsequently reduced by evaporation to 200-300 μL by gently blowing a stream of N₂ (g) over the liquid surface. The concentrated extract was injected to the same GC/MS as used for nicotine measurement, and the range of PAH concentration calibration was between 10 and 1000 pg/μL. Selected Ion Monitoring (SIM) was used for measuring the 27 PAHs listed in Table S4. Unfortunately, this method did not allow for the analysis of backing materials due to high background levels, and for that reason only top carpet layers were extracted and analyzed.

Section S5. Analysis of carpet-embedded chemicals using high resolution instruments

Chemical Ionization Mass Spectrometry. A portion of each carpet sample (~0.5 g) was placed in a glass flow tube at room temperature and heated to ~100°C using a Standard Dry Block Heater (Talboys) to vaporize the semi-volatile compounds on the carpet samples into the gas phase. Once the temperature stabilized at ~100°C, the volatilized compounds from the carpet were analyzed in real-time using an iodide-adduct Chemical Ionization Time-of-Flight Mass Spectrometer with a mass resolution ($m/\Delta m$) ~5000 (I-CIMS, Aerodyne Research Inc.) [3-7]. The I-CIMS is known to be sensitive for multifunctional O-containing and N-containing organic compounds [8-11]. Data processing was performed with Tofware (version 3.2.0., Tofwerk) running with Igor Pro (WaveMetrics, OR, USA). Only qualitative analysis could be conducted due to lack of internal standard, with tentative chemical identification made by elemental formula assignment.

Electrospray Ionization Mass Spectrometry. Carpet sample extracts were analyzed by direct infusion into an electrospray ionization high-resolution time-of-flight mass spectrometer (ESI-HR-TOF-MS, Agilent 6545 series). This instrument allows for accurate mass assignment over the range of m/z 30-1700 Da, within $\pm 5\%$ ppm of theoretical mass for the chemical formulas reported in this work. The ESI-HR-TOF-MS was operated in the positive ion mode and chemical formulas were assigned as $[M+H]^+$. Both the accurate mass and isotopic pattern were used to determine chemical formulas, corresponding to the Level 4 of identification confidence suggested by Schymanski et al. [12]. Data processing was performed with Agilent MassHunter Workstation Quantitative Analysis Software Version B.06.00, Build 6.0.633.0. Tentative chemical identifications were made based on the assignment of elemental formulas.

Table S2. Room-size chamber experiment timeline with sample time, airborne nicotine and total VOC (TVOC) concentration.

Sample name	Sampling start (d)	Airborne nicotine (ng m ⁻³)		TVOC (µg m ⁻³)	
		Sample duration (h)	Avg ± Error	Sample duration (h)	Avg ± Error
Chamber	-4.2	4.6	1.6 ± 0.2	4.8	34 ± 5
Chamber background ozonation t = - 29 h (Day -1.2); duration: 6 min					
Chamber ozonation	-0.3	5.1	2.8 ± 0.8	5.1	38 ± 5
Carpet installation t = 0 h (Day 0)					
Carpet background #1	2.7	6.7	29 ± 13	6.8	77 ± 11
Carpet background #2	4.7	47.4	19 ± 1	3.1	49 ± 7
Carpet background #3	5.0	46.9	18 ± 3	19.6	45 ± 6
Carpet background #4	9.7			6.0	55 ± 8
1st Carpet ozonation t = 240 h (Day 10.0); duration: 6 min					
1 st carpet ozonation #1	10.7	57.4	13 ± 3	6.4	53 ± 7
1 st carpet ozonation #2	11.0	68.9	17 ± 4	17.6	64 ± 9
1 st carpet ozonation #3	14.1			14.0	68 ± 10
2nd Carpet ozonation t = 402 h (Day 16.7); duration: 48 min					
2 nd carpet ozonation #1	17.0	47.6	9.0 ± 0.2	1.7	197 ± 24
2 nd carpet ozonation #2	17.1			15.9	139 ± 19
Smoking t = 456 h (Day 19.0)					
THS w/carpets	19.6	1.7	1168 ± 92	1.7	77 ± 10
3rd Carpet ozonation t = 473 h (Day 19.7); duration: 51 min					
3 rd carpet ozonation #1	20.0	18.7	101 ± 14	1.5	228 ± 30
3 rd carpet ozonation #2	20.1			15.6	167 ± 23
	30.9	67.4	44 ± 3		
3 rd carpet ozonation #3	33.0			16.7	63 ± 9
4th Carpet ozonation t = 809 h (Day 33.7); duration: 51 min					
4 th carpet ozonation #1	34.0	21.1	19 ± 3	1.6	210 ± 29
4 th carpet ozonation #2	34.1			15.4	178 ± 26

Table S3. Room-size chamber experiment timeline with sample time and carpet-bound nicotine loading concentration.

Sample name	Retrieval time (h)	Carpet nicotine loading (mg m ⁻²)			
		Top-X	Top-Y	Backing-X	Backing-Y
<i>Carpet installation t = 0 h</i>					
Carpet background	65.4	13	53	11	34
<i>1st ozonation t = 240 h</i>					
1 st carpet ozonation	257.0	28	84	17	38
<i>2nd ozonation t = 402 h</i>					
2 nd carpet ozonation	407.8	33	45	23	34
<i>Smoking t = 456 h</i>					
Post-smoking THS	471.5	30	94	46	30
<i>3rd ozonation t = 473 h</i>					
3 rd carpet ozonation	479.2	24	47	17	46
<i>4th ozonation t = 809 h</i>					
4 rd carpet ozonation	815.2	34	70	13	45

Section S6. Measurement of gas phase species and aerosols in room-sized chamber

Nicotine by the Hammond method. Airborne nicotine was actively sampled in duplicate with 47 mm A/E glass fiber filters (Pall) coated with sodium bisulfate, housed in open face filter holders. Air pumps (Leland Legacy, SKC Inc) pulled air through the filters at a flow rate of 5-10 L min⁻¹ with a sample duration of 3.3 - 69 h. After collection, the filter samples were stored in plastic petri dishes at -4 °C until being delivered to UC Berkeley for analysis. The filters were analyzed with the collected nicotine and bisulfate desorbed in a solution of 95% water and 5% methanol. The pH was adjusted with 10 N sodium hydroxide, and the neutral nicotine molecule was concentrated into 500 µL of ammoniated heptane by liquid-liquid extraction. An aliquot of the heptane solution was injected into an Agilent 7820 Gas Chromatograph with an Agilent 5977 Mass Spectrometer Detector for quantitation of nicotine. The range of nicotine standard concentration was 0.01 µg mL⁻¹ to 10 µg mL⁻¹ for the GCMS method calibration. The reported uncertainty was calculated as the difference of the duplicate determinations.

Volatile organic compounds (VOCs). VOCs were collected onto Carboxen sorbent tubes (Supelco). Quantification of terpenoids and their degradation byproducts was carried out by thermal desorption gas chromatography mass spectrometry (TD-GC/MS) using bromofluorobenzene as an internal standard, following an established EPA method [13]. An Agilent GC/MS system (model 6890/5973) was operated in electron impact mode, and was interfaced with a thermal desorption inlet with an autosampler (Gerstel). Calibration curves were created for 44 VOCs for which authentic standards were available, including hexanal, nonanal, phenol, d-limonene, tetradecane, dodecane, octanal, butanal, decanal, heptanal, 2-ethyl-1-hexanol, isobutyrate (txib mono-isomer), cyclotetrasiloxane, toluene, benzaldehyde, α-pinene, 2-butoxyethanol, cyclopentasiloxane, benzene, kodaflex TXIB, hexane, m/p-xylene, heptane, octane, hexadecane, diethyl phthalate, naphthalene, ethylbenzene, o-xylene, trichloromethane, 1,2,4-trimethylbenzene, decane, styrene, undecane, 3-carene, α-terpineol, tetrachloroethylene, dimethyl phthalate, 1,2,3-trimethylbenzene, dibutyl phthalate, 1,4-dichlorobenzene, butylbenzene, g-terpinene, and hexamethylcyclotrisiloxane. When standards were not commercially available, the compounds were tentatively identified through a NIST database and quantified via a surrogate compound (toluene). Blank chamber measurements were also performed prior to heating the mixtures, to subtract background levels when applicable. The reported values are the average of two duplicate determinations. Experimental uncertainties were estimated as the absolute difference of those duplicates.

Volatile carbonyls. Low MW aldehydes and ketones were collected onto duplicate dinitrophenylhydrazine (DNPH)-impregnated cartridges collected simultaneously with the VOC samples.

The collected DNPH cartridges were extracted with 2 mL of carbonyl-free acetonitrile (Honeywell) and analyzed by high performance liquid chromatography (HPLC) with UV detection (Agilent 1200), following the EPA TO-11 method [14]. A certified mixture of DNPH derivatives was obtained from Sigma-Aldrich as standards for analysis of formaldehyde, acetaldehyde, acrolein, acetone, propanal, crotonaldehyde, methacrolein, butanal, 2-butanone, benzaldehyde, m-tolualdehyde, and hexaldehyde. Calibration curves were generated for quantification of each analyte using those standards. Chamber blank measurements were subtracted from the values obtained for the samples. The reported values are the average of two duplicate determinations. Experimental uncertainties were estimated as the absolute difference of those duplicates.

Ozone. In bench-scale and room-sized experiments, the ozone concentration was recorded in real time with a 10-second sampling frequency, using a photometric detector (2BTech Model 202).

Particulate matter. Sampling of aerosols formed in the chamber during the heating process was carried out with three instruments operating simultaneously: a Fast Mobility Particle Sizer (FMPS) spectrometer (Model 3091, TSI Inc., MA), an Aerodynamic Particle Sizer (APS) spectrometer (Model 3321, TSI Inc., MA), and an Optical Particle Sizer (OPS) (Model 3330, TSI Inc., MA). The FMPS measures particles with diameters between 8 and 300 nm with 1 Hz resolution, allowing for fast measurement of quickly evolving aerosols such as those generated in these experiments. The other two instruments expanded the PM size range up to 2500 nm with additional 23 size bins. Mass distribution of particles was calculated by assuming particle density as 1 g cm^{-3} .

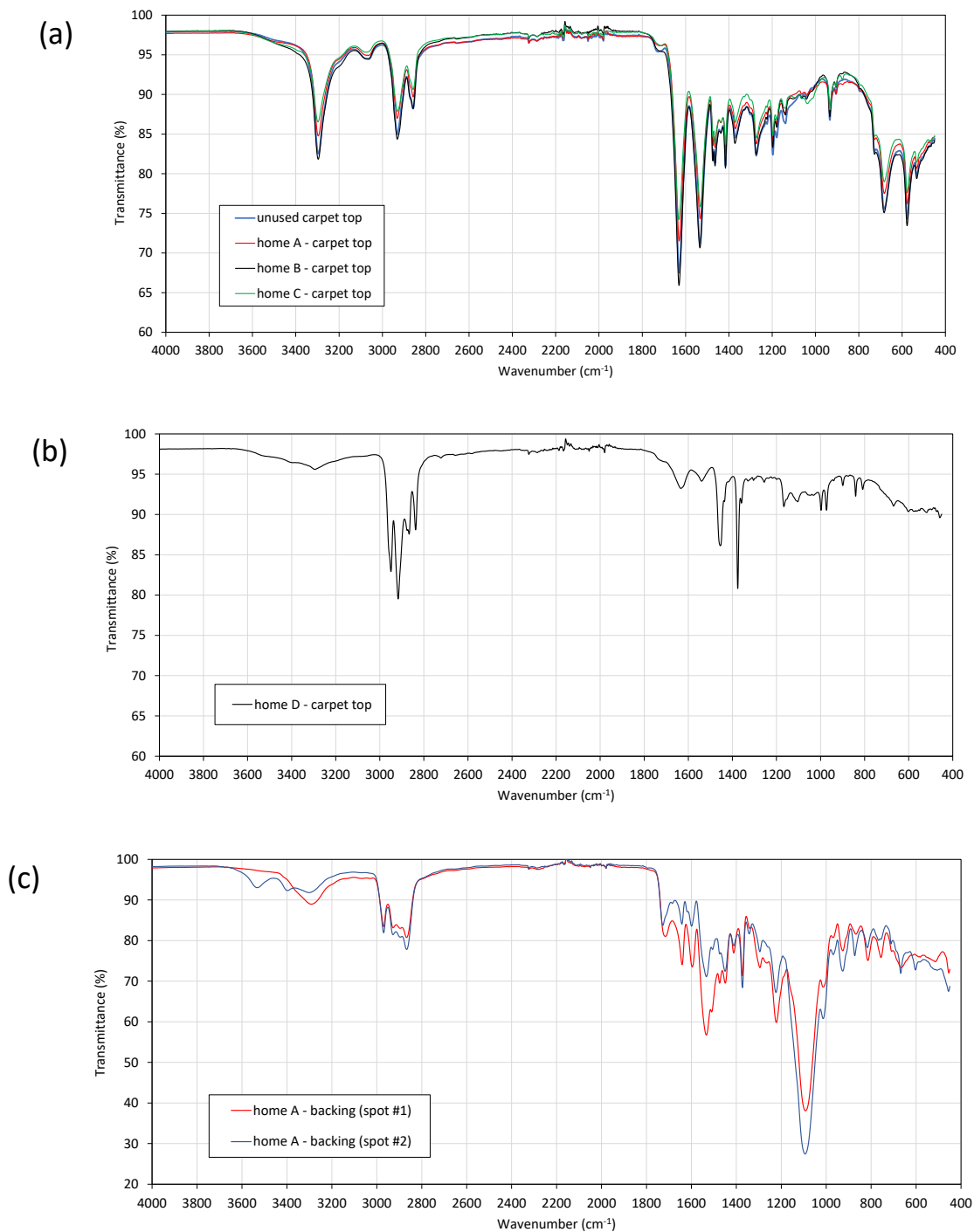


Figure S5. ATR-FTIR spectra corresponding to (a) carpet top specimens consistent with nylon fibers; (b) carpet top specimen consistent with polypropylene fibers; (c) two spots in a backing specimen consistent with polyurethane foam.

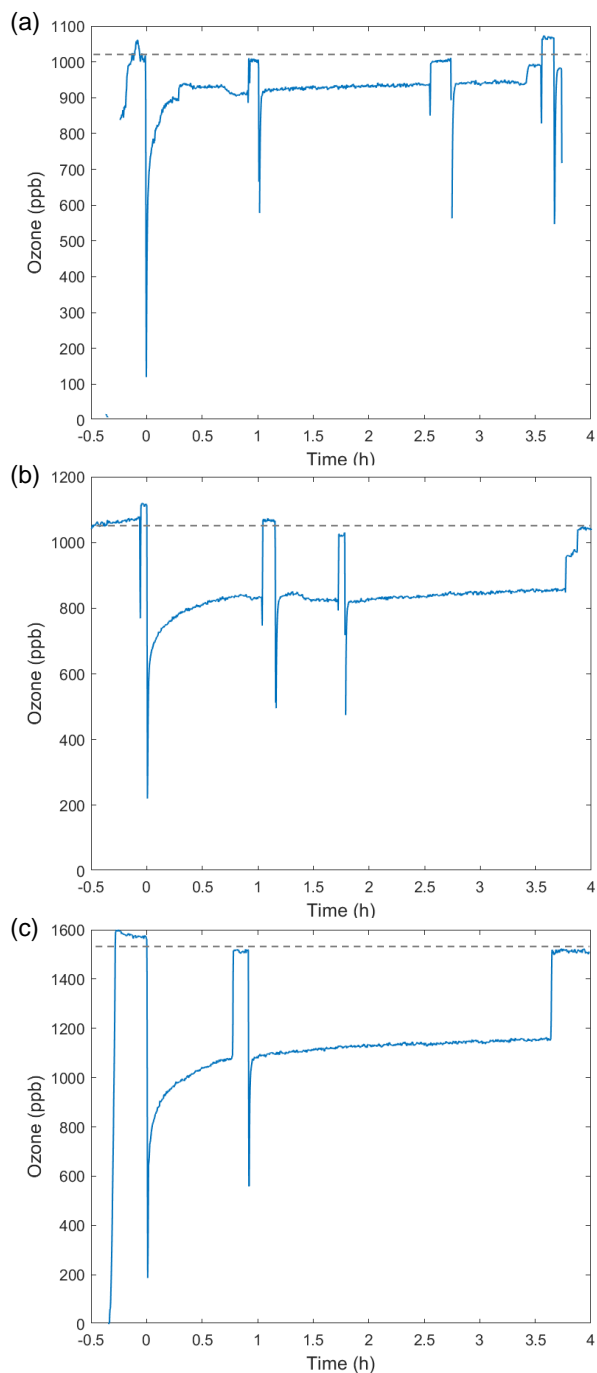


Figure S6. Ozone concentration in bench-scale experiments with (a) unexposed new carpet; (b) fresh THS on clean carpet; and (c) aged THS on field carpet from home B. Dotted lines indicate the baseline ozone level.

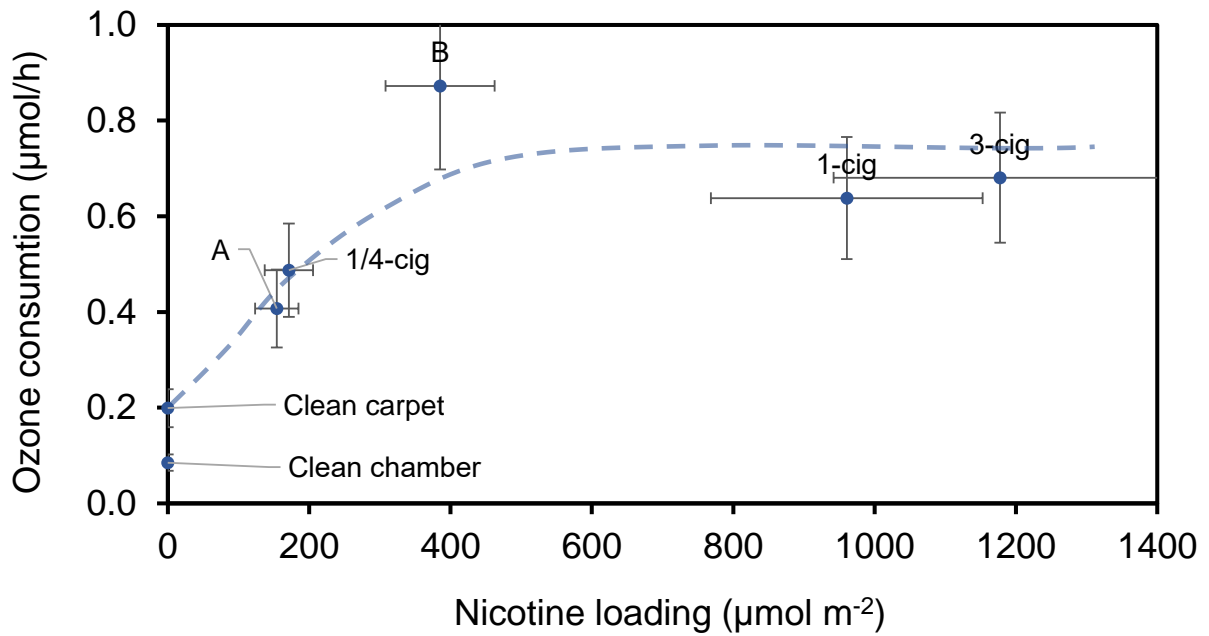


Figure S7. Ozone consumption rate as a function of nicotine loading on different carpet specimens.

Table S4. PAH concentrations measured from carpet specimens, and removal efficiency after ozonation in the bench-scale chamber.

Acronym	Name	MW	Formula	CAS #	VP@ 25C (mm Hg)	Carpet top loading, PAH ₀ ($\mu\text{g m}^{-2}$)			Removal efficiency, RE_{PAH}^i	
						No THS	3-Cig	Carpet B	3-Cig	Carpet B
NAP	naphthalene	128.2	C10H8	91-20-3	9 E-2	21	172	288	N.R.	N.R.
1-MN	1-methyl naphthalene	142.2	C11H10	90-12-0	7 E-2	6.5	201	197	N.R.	N.R.
2-MN	2-methylnaphthalene	142.2	C11H10	91-57-6	6 E-2	4.8	222	123	N.R.	N.R.
ACE	Acenaphthylene	152.2	C12H8	208-96-8	5 E-3	3.0	44	38	N.R.	N.R.
FLU	fluorene	166.2	C13H10	86-73-7	6 E-4	4.9	21	49	8%	28%
PHEN	phenanthrene	178.2	C14H10	85-01-8	1 E-4	36	179	1361	20%	12%
ANCE	Anthracene	178.2	C14H10	120-12-7	6 E-6	0.7	10	79	45%	45%
1-M-PHEN	1-methylphenanthrene	192.3	C15H12	832-69-9	5 E-5	8.2	55	304	37%	43%
2-M-PHEN	2-methylphenanthrene	192.3	C15H12	2531-84-2	5 E-5	14	70	318	24%	42%
3-M-PHEN	3-methylphenanthrene	192.3	C15H12	832-71-3	5 E-5	10	66	335	38%	45%
FLNT	fluoranthene	202.3	C16H10	206-44-0	9 E-6	7.6	35	75	32%	60%
PYR	pyrene	202.3	C16H10	129-00-0	4 E-6	10	36	68	24%	53%
7H-B[c]FLN	7H-Benzo[c]fluorene	216.3	C17H12	205-12-9	N/A	18	27	89	9%	55%
C[cd]P	Cyclopenta[cd]pyrene	226.3	C18H10	27208-37-3	N/A	16	32	86	N.R.	N.R.
B[a]A	Benz[a]anthracene	228.3	C18H12	56-55-3	2 E-7	< LOQ	37	80	16%	37%
CRY	chrysene	228.3	C18H12	218-01-9	6 E-9	16	34	141	13%	11%
5-MCRY	5-methylchrysene	242.3	C19H14	3697-24-3	5 E-7	11	26	280	34%	79%
B[b]F	Benzo[b]fluoranthene	252.3	C20H12	205-99-2	5 E-7	< LOQ	25	16	100%	61%
B[e]P	Benzo[e]pyrene	252.3	C20H12	192-97-2	5 E-9	1.0	2.0	17	N.R.	47%
B[a]P	Benzo[a]pyrene	252.3	C20H12	50-32-8	5 E-9	1.7	5.7	31	80%	45%
B[k]F	Benzo[k]fluoranthene	252.3	C20H12	207-08-9	9 E-10	12	174	107	16%	65%
D[a,h]A	Dibenz[a,h]anthracene	278.3	C22H14	53-70-3	9 E-10	1.4	3.3	4.4	N.R.	N.R.
I[1,2,3-c]PYR	Indeno[1,2,3-c]pyrene	276.3	C22H12	193-39-5	1 E-10	8.7	20	13	N.R.	87%
B[ghi]PR	Benzo[ghi]perylene	276.3	C22H12	191-24-2	1 E-10	0.6	4.3	34	55%	81%
COR	Coronene	300.4	C24H12	191-07-1	N/A	0.7	1.4	16	97%	71%
D[a,e]P	Dibenzo[a,e]pyrene	302.4	C24H14	192-65-4	5 E-11	6.1	12	< LOQ	12%	N.R.
D[a,l]P	Dibenz[a,l]pyrene	302.4	C24H14	189-55-9	2 E-11	26	37	137	15%	100%
	TOTAL PAH					246	1552	4286		

N/A: not available; <LOQ: below the limit of quantification; N.R.: not reported

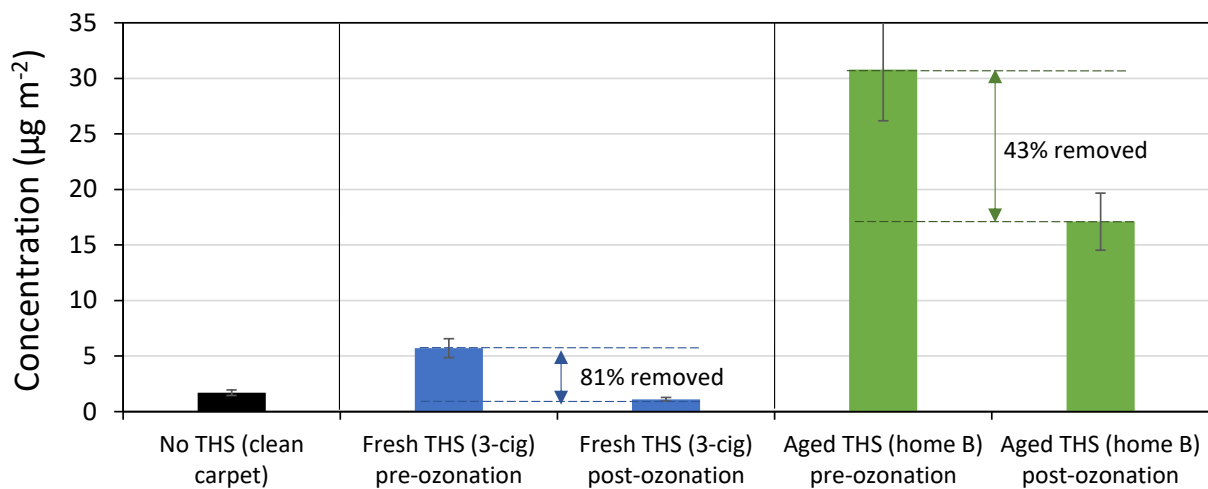


Figure S8. Concentration of Benzo[a]pyrene measured in THS-free samples of clean carpet, in freshly deposited THS, and aged THS in a carpet retrieved from home B.

Table S5. Results from ESI-MS and CIMS analysis

MW	Assigned formula	Possible species	Possible source	Fresh THS (3-cig) on carpet		Field carpet	
				CIMS	ESI-MS	CIMS	ESI-MS
162.12	C ₁₀ H ₁₄ N ₂	Nicotine	Tobacco-related		Pre, Post		Pre, Post
176.22	C ₁₀ H ₁₂ N ₂ O	Cotinine		Pre, Post		Pre, Post	Pre, Post
178.22	C ₁₀ H ₁₄ N ₂ O	Nicotine N-oxide		Pre, Post		Pre, Post	Pre, Post
122.12	C ₆ H ₆ N ₂ O	Nicotinamide		Pre, Post		Pre, Post	Pre, Post
59.07	C ₂ H ₅ NO	N-methylformamide		Pre, Post		Pre	
123.11	C ₆ H ₅ NO ₂			Pre, Post	Pre, Post	Pre, Post	Pre, Post
136.15	C ₇ H ₈ N ₂ O	Nicotinyl methylamide		Pre, Post	Pre, Post	Pre, Post	Pre, Post
161.22	C ₁₀ H ₁₃ N ₂	Nicotine imine		Pre, Post		Pre, Post	
163.17	C ₉ H ₉ NO ₂			Pre, Post		Pre, Post	
164.20	C ₉ H ₁₂ N ₂ O			Pre, Post		Pre, Post	
226.18	C ₁₂ H ₂₂ N ₂ O ₂	Nylon cyclic dimer	Nylon oxidation		Pre, Post		Pre, Post
422.44	C ₁₃ H ₃₀ N ₁₀ O ₆						Post
718.89	C ₂₉ H ₆₂ N ₁₄ O ₇						Post
746.94	C ₃₁ H ₆₆ N ₁₄ O ₇						Post
266.40	C ₁₂ H ₂₆ O ₄ S	Dodecyl sulfate	Cooking, household products				Pre, Post
256.42	C ₁₆ H ₃₂ O ₂	Palmitate					Pre, Post
284.48	C ₁₈ H ₃₆ O ₂	Stearate					Pre, Post

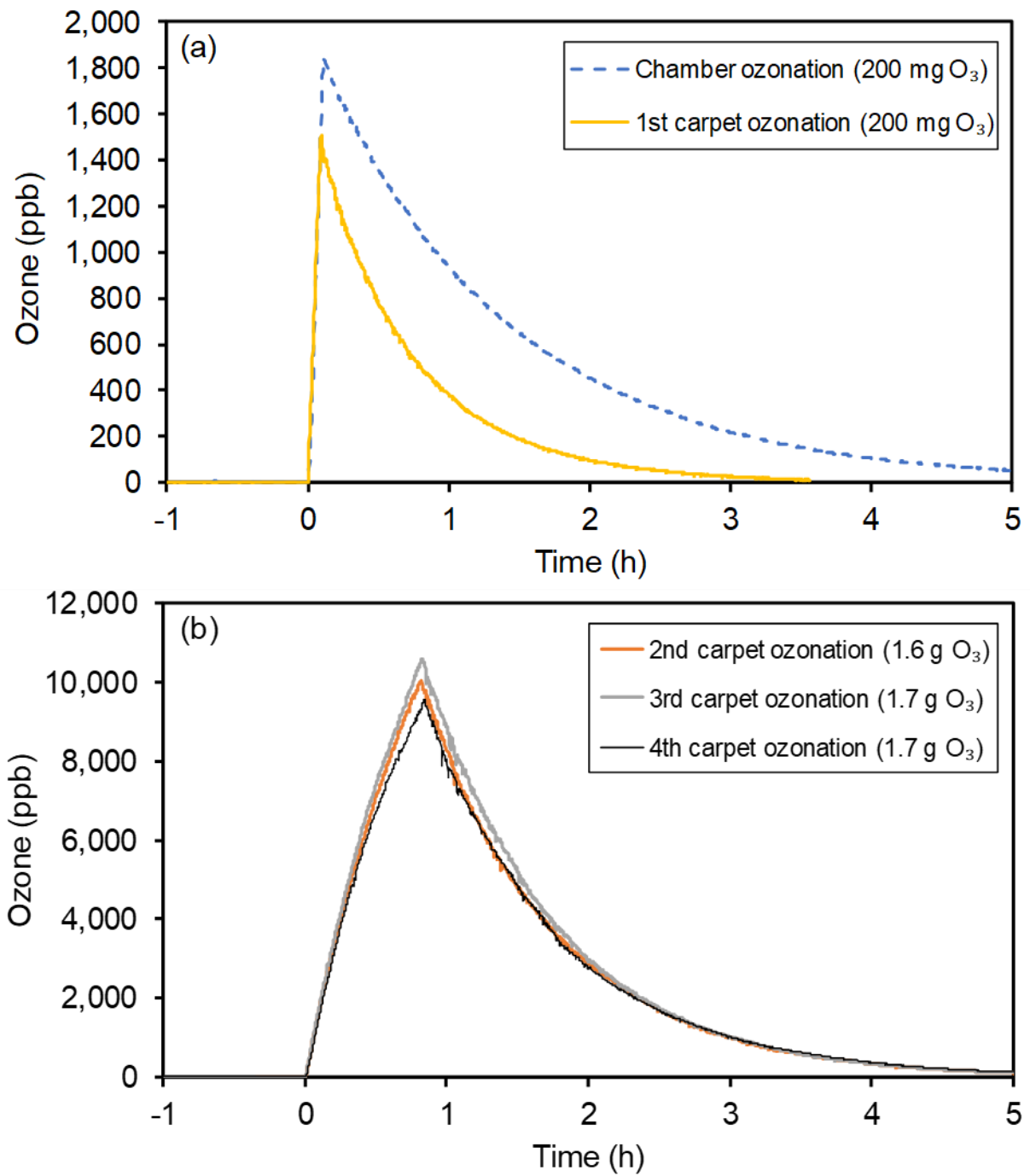


Figure S9. Ozone concentration during five room-sized chamber ozonation experiments. (a) initial tests with relatively low ozone dose; (b) subsequent tests with higher ozone dose.

Table S6. Emission rates (expressed in $\mu\text{g h}^{-1} \text{m}^{-2}$) of the four most abundant carbonyls in the room-size chamber ozonation experiment. Emissions were recorded approximately six hours after ozonation ended, in experiments where 1.6 – 1.7 g ozone were released during 48 – 51 min.

Carbonyl	2 nd carpet ozonation	3 rd carpet ozonation	4 th carpet ozonation	Average of the three determinations
Nonanal	71	112	94	92 ± 21
Hexanal	59	53	44	52 ± 8
Acetone	45	39	19	34 ± 14
Formaldehyde	20	29	23	24 ± 5

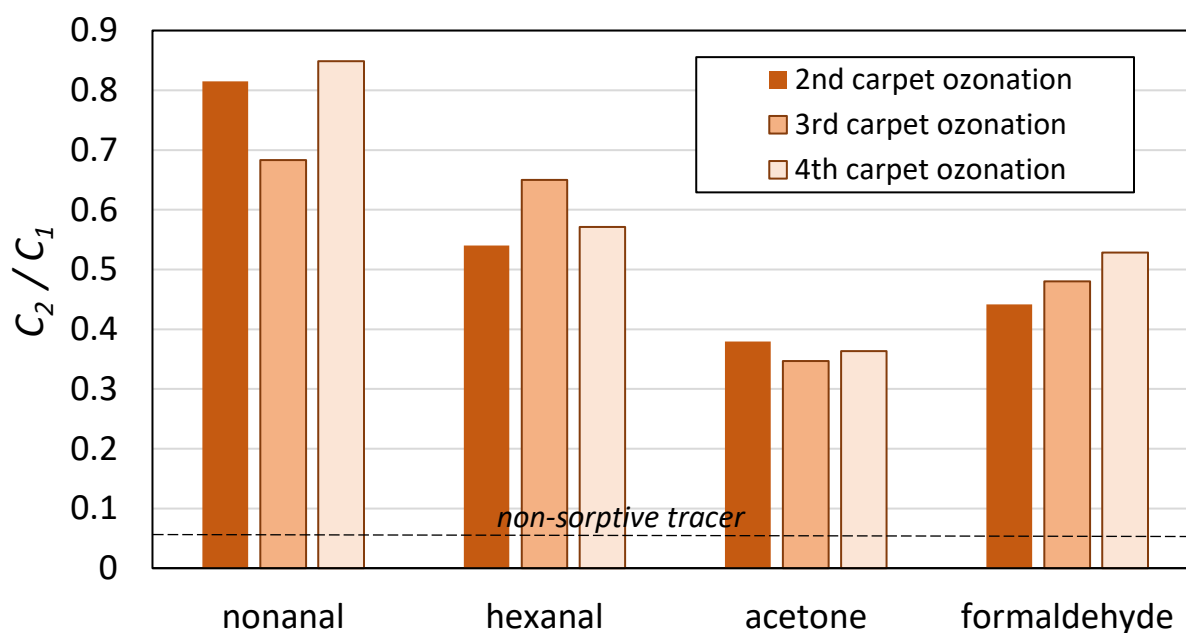


Figure S10. Ratio between aldehyde concentration measured in the second and first VOC sample, for each of the high-dose carpet ozonation tests. The dotted line represents the ratio estimated for a non-sorptive tracer being removed by ventilation during the same period.

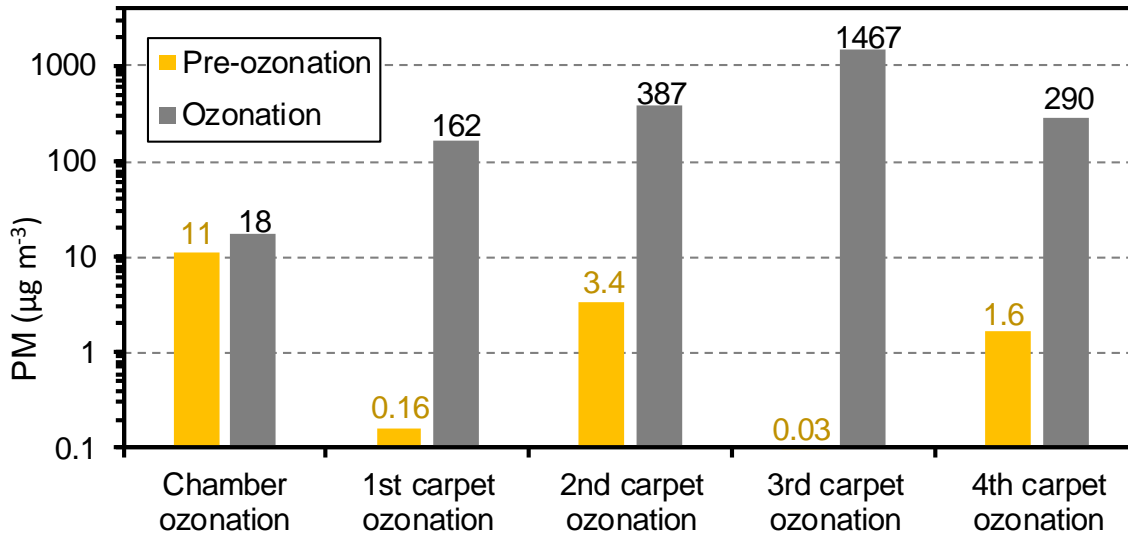


Figure S11. Peak particle mass concentration ($\mu\text{g m}^{-3}$) calculated for each ozonation experiment from FMPS measurement, assuming particle density is 1 g cm^{-3} .

Table S7. Nicotine emission rates predicted from our room-sized chamber, and reported in the literature

Nicotine emission rate	Conditions	Reference
<i>Carpet emissions</i>		
47 – 95 $\mu\text{g day}^{-1}$	Assuming 50 – 100 m ² carpet in smoker's home	(this study)
<i>Regular cigarettes - Mainstream smoke emissions</i>		
0.6 – 2 mg cig ⁻¹	US cigarettes by FTC method	[15]
0.83 – 0.95 mg cig ⁻¹	US cigarettes by FTC method	[16]
2 \pm 0.1 mg cig ⁻¹	European cigarettes by Health Canada Intense (HCI) method	[17]
0.2 – 1.8 mg cig ⁻¹	Japanese cigarettes by ISO method	[18]
0.9 – 2.2 mg cig ⁻¹	Japanese cigarettes by HCI method	[18]
0.75 – 0.85 mg cig ⁻¹	Lebanese cigarettes y ISO method	[19]
1.69 – 1.91 mg cig ⁻¹	Lebanese cigarettes by HCI method	[20]
<i>Regular cigarettes – Sidestream smoke emissions</i>		
4.5 – 6.1 mg cig ⁻¹	US cigarettes	[16]
<i>Regular cigarettes – Environmental tobacco smoke (ETS) emissions</i>		
1.59 mg cig ⁻¹	Average of 50 leading US brand/style cigarettes	[20]
<i>Heat-not-burn cigarettes – Mainstream emissions</i>		
1.3 – 1.5 mg cig ⁻¹	European HnB cigarettes by HCI method	[17]
0.71 – 0.83 mg cig ⁻¹	IQOS by ISO method	[19]
1.3 – 1.7 mg cig ⁻¹	IQOS by HCI method	[19]

References

1. Quintana, P.J.; Matt, G.E.; Chatfield, D.; Zakarian, J.M.; Fortmann, A.L.; Hoh, E. Wipe sampling for nicotine as a marker of thirdhand tobacco smoke contamination on surfaces in homes, cars, and hotels. *Nicotine Tob. Res.* 2013, 15(9), 1555-63. <https://doi.org/10.1093/ntr/ntt014>.
2. Matt, GE; Quintana, PJE; Hoh, E; Zakarian, JM; Dodder, NG; Record, RA; Hovell, MF; Mahabee-Gittens EM; Padilla S; Markman L; Watanabe K; Novotny TE. Remediating Thirdhand Smoke Pollution in Multiunit Housing: Temporary Reductions and the Challenges of Persistent Reservoirs. *Nicotine Tob. Res.* 2021, 23: 364–372. <https://doi.org/10.1093/ntr/ntaa151>.
3. Zhao, Z.; Xu, Q.; Yang, X.; Zhang, H. Heterogeneous Ozonolysis of Endocyclic Unsaturated Organic Aerosol Proxies: Implications for Criegee Intermediate Dynamics and Later-Generation Reactions. *ACS Earth Space Chem.* 2019, 3 (3), 344–356. <https://doi.org/10.1021/acsearthspacechem.8b00177>.
4. Mayorga, R.; Xia, Y.; Zhao, Z.; Long, B.; Zhang, H. Peroxy Radical Autoxidation and Sequential Oxidation in Organic Nitrate Formation during Limonene Nighttime Oxidation. *Environ. Sci. Technol.* 2022, 56 (22), 15337–15346. <https://doi.org/10.1021/acs.est.2c04030>.
5. Zhao, Z.; Zhang, W.; Alexander, T.; Zhang, X.; Martin, D. B. C.; Zhang, H. Isolating α -Pinene Ozonolysis Pathways Reveals New Insights into Peroxy Radical Chemistry and Secondary Organic Aerosol Formation. *Environ. Sci. Technol.* 2021, 55 (10), 6700–6709. <https://doi.org/10.1021/acs.est.1c02107>.
6. Zhang, W.; Zhang, H. Secondary Ion Chemistry Mediated by Ozone and Acidic Organic Molecules in Iodide-Adduct Chemical Ionization Mass Spectrometry. *Anal. Chem.* 2021, 93 (24), 8595–8602. <https://doi.org/10.1021/acs.analchem.1c01486>.
7. Zhao, Z.; Tolentino, R.; Lee, J.; Vuong, A.; Yang, X.; Zhang, H. Interfacial Dimerization by Organic Radical Reactions during Heterogeneous Oxidative Aging of Oxygenated Organic Aerosols. *J. Phys. Chem. A* 2019, 123 (50), 10782–10792. <https://doi.org/10.1021/acs.jpca.9b10779>.
8. Lee, B. H.; Mohr, C.; Lopez-Hilfiker, F. D.; Lutz, A.; Hallquist, M.; Lee, L.; Romer, P.; Cohen, R. C.; Iyer, S.; Kurtén, T.; Hu, W.; Day, D. A.; Campuzano-Jost, P.; Jimenez, J. L.; Xu, L.; Ng, N. L.; Guo, H.; Weber, R. J.; Wild, R. J.; Brown, S. S.; Koss, A.; de Gouw, J.; Olson, K.; Goldstein, A. H.; Seco, R.; Kim, S.;

- McAvey, K.; Shepson, P. B.; Starn, T.; Baumann, K.; Edgerton, E. S.; Liu, J.; Shilling, J. E.; Miller, D. O.; Brune, W.; Schobesberger, S.; D'Ambro, E. L.; Thornton, J. A. Highly Functionalized Organic Nitrates in the Southeast United States: Contribution to Secondary Organic Aerosol and Reactive Nitrogen Budgets. *Proc Natl Acad Sci USA* 2016, *113* (6), 1516–1521. <https://doi.org/10.1073/pnas.1508108113>.
9. Iyer, S.; He, X.; Hyttinen, N.; Kurtén, T.; Rissanen, M. P. Computational and Experimental Investigation of the Detection of HO₂ Radical and the Products of Its Reaction with Cyclohexene Ozonolysis Derived RO₂ Radicals by an Iodide-Based Chemical Ionization Mass Spectrometer. *J. Phys. Chem. A* 2017, *121* (36), 6778–6789. <https://doi.org/10.1021/acs.jpca.7b01588>.
10. Mohr, C.; Lopez-Hilfiker, F. D.; Yli-Juuti, T.; Heitto, A.; Lutz, A.; Hallquist, M.; D'Ambro, E. L.; Rissanen, M. P.; Hao, L.; Schobesberger, S.; Kulmala, M.; Mauldin, R. L.; Makkonen, U.; Sipilä, M.; Petäjä, T.; Thornton, J. A. Ambient Observations of Dimers from Terpene Oxidation in the Gas Phase: Implications for New Particle Formation and Growth: Ambient Observations of Gas-Phase Dimers. *Geophys. Res. Lett.* 2017, *44* (6), 2958–2966. <https://doi.org/10.1002/2017GL072718>.
11. Zhang, X.; Lambe, A. T.; Upshur, M. A.; Brooks, W. A.; Gray Bé, A.; Thomson, R. J.; Geiger, F. M.; Surratt, J. D.; Zhang, Z.; Gold, A.; Graf, S.; Cubison, M. J.; Groessl, M.; Jayne, J. T.; Worsnop, D. R.; Canagaratna, M. R. Highly Oxygenated Multifunctional Compounds in α -Pinene Secondary Organic Aerosol. *Environ. Sci. Technol.* 2017, *51* (11), 5932–5940. <https://doi.org/10.1021/acs.est.6b06588>.
12. Schymanski EL, Jeon J, Gulde R, Fenner K, Ruff M, Singer HP, Hollender J. Identifying small molecules via high resolution mass spectrometry: Communicating confidence. *Environ. Sci. Technol.* 2014, *48*, 2097-2098. DOI: 10.1021/es5002105
13. US EPA. Method TO-1, Revision 1.0. Method for the Determination of Volatile Organic Compounds in Ambient Air Using Tenax[®] Adsorption and Gas Chromatography/Mass Spectrometry (GC/MS). Center for Environmental Research Information, Office of Research and Development, Cincinnati, OH, 1984.
14. US EPA. Compendium Method TO-11A. Determination of Formaldehyde in Ambient Air Using Adsorbent Cartridge Followed by High Performance Liquid Chromatography (HPLC). Center for Environmental Research Information Office of Research and Development: Cincinnati, OH, 1999.

15. Borgerding, M. F.; Perfetti, T. A.; Ralapati, S. Chapter 9 – Determination of nicotine in tobacco, tobacco processing environments and tobacco products. In Gorrod JW and Jacob P III, *Analytical determination of nicotine and related compounds and their metabolites*. Elsevier, Amsterdam, 1999.
16. Rustemeier, K.; Piade J. J. Chapter 12 – Determination of nicotine in mainstream and sidestream cigarette smoke. In Gorrod JW and Jacob P III, *Analytical determination of nicotine and related compounds and their metabolites*. Elsevier, Amsterdam, 1999.
17. Farsalinos, KE.; Yannovits, N.; Sarri, T., Voudris, V.; Poulas, K. Nicotine delivery to the aerosol of a heat-not-burn tobacco product: Comparison with a tobacco cigarette. *Nic. Tob. Res.* 2018, 1004-1009. DOI: 10.1093/ntr/ntx138
18. Endo, O.; Matsumoto, M.; Inaba, Y.; Sugita, K.; Nakajima, D.; Goto, S.; Ogata, H.; Suzuki, G. Nicotine, tar, and mutagenicity of mainstream smoke generated by machine smoking with International Organization for Standardization and Health Canada Intense regimens of major Japanese cigarette brands. *J. Health Sci.* 2009, 55(3), 421-427.
19. Salman, R.; Talih S.; El-Hage, R.; Haddad, C.; Karaoghlanian, N.; El-Hellani, A.; Saliba, N.A.; Shihadeh, A. Free-base and total nicotine, reactive oxygen species, and carbonyl emissions from IQOS, a heated tobacco product. *Nic. Tob. Res.* 2019, 1285-1288. DOI: 10.1093/ntr/nty235
20. Ogden, M.W.; Jenkins, R.A. Chapter 13 - Nicotine in environmental tobacco smoke. In Gorrod JW and Jacob P III, *Analytical determination of nicotine and related compounds and their metabolites*. Elsevier, Amsterdam, 1999.